UNIVERSITÉ DE GENÈVE

INSTITUT DES SCIENCES DE L'ENVIRONNEMENT

Certificat complémentaire de Géomatique 2019

Mémoire de Stage at GRID-GENEVA

Swiss Data-Cube: the potential for monitoring wet snow cover in Alpine environment using SAR remote sensing C-band images from Sentinel-1 mission.

Marzia Carolini

January 2020
University of Geneva, Switzerland

Director: Dr. Gregory Giuliani

Table of contents

Table of tables

Table of Figures

1. Abstract :

Synthetic Aperture Radar (SAR) is a valuable technology to monitoring the wet snow cover extent in mountain regions. This study focuses on Alpine environment in Europe where seasonal wet snow cover is essential for the hydrology and water management. A Sentinel-1 time series of Ground Range Detected (GRD) radar images generated by the Interferometric Wide Swath (IW) sensor mode have been downloaded from the Copernicus Open Access Hub web site. Data set covers from January 2019 to the end of June 2019; they have been radiometrically terrain corrected (RTC) and manipulated to analyse the gamma coefficient backscatter and detect the melting process of the wet snow cover in the Alps. Results show the seasonal melting process in the study area starting from March, reaching its maximum on May, and continuing in June with an evaporation event. Changes in snow pack are presented through the spatial distribution in the dB images where wet snow cover appears through darker pixels, while the dry snow pack and the bare ground appear with brighter pixels; and through the transformations of the backscatter values in the histograms. An RGB composition has also been presented to show the difference between the chosen periods of the year (i.e. January, April and June). Finally, binary wet snow cover maps have been created to show seasonal changes in water content in the snow pack. The analysis presents the potential for SAR C-band S1A satellite in detecting the wet snow cover in mountain regions. However, improvements can be made by integrating other forms of data to be compared with the SAR remote sensing results in order to provide more accuracy, e.g. other satellites' data or field work datasets.

2. GRID-Geneva :

Born from the partnership among the United Nations Environment Programme (UNEP), the Swiss Federal Office for the Environment (FOEN) and the University of Geneva (UniGe), the Global Resource Information Database - Geneva (GRID-Geneva) has the objective of monitoring environmental issues and phenomena by transforming data in useful information and knowledge in order to support the decision-making process concerning the environment [1].

Experts in the GRID-Geneva are trained to process satellite imagery with remote sensing software, to build models from geospatial data applying Geographical Information Systems (GIS) methods and techniques and, finally, they produce interactive maps and graphs to better share information.

Through the partnership with the UNEP and the FOEN, GRID-Geneva is engaged in supporting capacity building and teaching about environmental issues in different countries around the world. Scientists of GRID-Geneva provide conferences and workshop meeting to share knowledge and information by assisting the decision-making process.

While, by the partnership with the UniGe, the GRID-Geneva contributes in teaching GIS at the University by introducing and training students towards geomatics and environmental concerns.

3. Introduction :

Europe is severely affected by global warming effects and it is experiencing glaciers and permanent snow to melt in the Alps regions, seeing them to be gone forever. Wet snow cover extent (SCE) seasonality has significant impacts on the hydrology of this regions, affecting tourism and landscapes, electricity generation from hydropower; and generating concerns about risks of runoff and avalanches.

Considering global warming contribution to enhance melting process in the Alps, this analysis aims to observe an intra-annual change of the wet snow cover. Wet snow cover is becoming an essential parameter to observe how much the region is affected. In fact, in mountain regions, the wet snow covers determines an important element in risk and disaster management and it also contributes in agriculture management, essential for the local economy.

This is a remote sensing analysis based on the detection and manipulation of radar images generated by the satellite Sentinel-1A and the purpose is to analyse and describe the changes in the backscattered gamma values of the study area.

3.1. Wet snow cover in Swiss Alpine environment:

Glaciers and snow cover are essential in Alpine environment because they supply fresh water to all Europe continent. Switzerland has been called for centuries “the water tower” of Europe due to the presence of around 40 glaciers and an important extend of permanent and seasonal snow cover. However, due to global warming, glaciers are melting, and the permanent snow cover is reducing, increasing the seasonal snow cover, known as “wet snow cover”. Since wet snow cover plays a significant role in the risk and disaster assessments, hydrology and water management of the region, environmental monitoring is becoming crucial for preventing flooding, avalanches and other climate change related issues. In fact, Swiss Alps are highly dense in population and debris flows and avalanches could be significantly dangerous. Therefore, a good knowledge about the seasonal distribution of the wet snow cover, and its length, is the first step to prevent risks and disasters.

Although terrain-based measurements are still useful to get information about the seasonality of the wet snow cover, technological innovation has encouraged remote sensing by the means of airplane, at first, then artificial satellites and probably soon by using drones. Environmental monitoring using the visible section of the electromagnetic spectrum has proven to be effective in mapping the snow cover using the Normalized Difference Snow Index (NDSI), nevertheless, this index failed in making the difference between the dry and the wet portion of snow cover [2].

Despite this, studies related to low frequencies of the electromagnetic radiation have demonstrated that microwaves are, instead, effective in detecting the water content of a target and the roughness of surfaces. Since microwaves can detect targets under every-condition weather, they are not affected by clouds and do not depend on external radiation, i.e. they can be used to detect objects in both day and night time and resulting images do not need atmospheric correction [2]. Microwaves are characterized by frequencies in GHz and wavelength ranged from millimetres (mm) to meters (m). These characteristics make RADAR (Radio Detection And Ranging) technology the best suitable option to detect and mapping wet snow cover.

3.2. Remote sensing and SAR images processing :

Since 60's, remote sensing has been used to monitoring environmental phenomena and Earth's spheres, i.e. atmosphere, geosphere, hydrosphere and biosphere, from the outside space by means of satellite-based sensor technologies [3]. According to the American Society for Photogrammetry and Remote Sensing's definition, remote sensing allows to get reliable information about objects and the environment "through the process of recording, measuring and interpreting imagery and digital representations of energy patterns" derived with these sensor systems [4].

Sensors can be active or passive: they can provide their own source of electromagnetic energy to illuminate the objects they observe; or they can rely on an external source of radiation, like sunlight, and collect the amount of radiation which is reflected or backscattered by the target.

The Synthetic Aperture Radar (SAR) is an active radio detection sensor which transmits, from an antenna, some electromagnetic pulses and receives the echoes of the backscattered signal [5]–[7] It can precisely identify the target distance and distinguish objects on the ground, by measuring the time difference between the transmitted pulse and the reflected one (i.e. Doppler effect).

SAR has been often used to detect temporal and spatial changes in snow cover extent (SCE) because it provides day-and-night high-resolution two-dimensional images which are independent from weather conditions and clouds [5][7]. Moreover, it is sensitive to dielectric properties of targets (water content, humidity) and to its roughness; so, it can easily detect their moisture and roughness; and it is related to the acquisition geometry, providing information about the topography. It can distinguish an object's moisture content, salinity and physical characteristics, such as shape, size and orientation through microwave pulses [8]–[11].

Microwave portions of the spectrum are often referenced using both wavelength and frequency [5]. Microwaves can penetrate targets depending on their wavelength: L-band ($\lambda = 23$ cm) has the higher penetration capabilities and reaches 20 m of depth, C-band ($\lambda = 6$ cm) reaches 6 m of depth and the X-band ($\lambda = 3$ cm) gets to 1 m of depth. However, the choice of the wavelength depends on the objective of the analysis. For SCE detection and mapping, the C-band is the most commonly used wavelength [9]. In addition, another important SAR aspect is polarization, which refers to the orientation of the electric field. Microwave radiation can be transmitted either horizontally (H) or vertically (V) and the receiving antenna can even record both together, i.e. combinations of polarizations are like-polarized (HH and VV) or cross-polarized (HV and VH) [5].

So, SAR has a great potential in detecting dry and wet snow cover because when the target has high moisture content, signals would be weaker because they cannot penetrate it. The reflected signals are often lower from areas covered with wet-snow, compared to snow-free or dry snow [11].

3.3. Sentinel-1 :

In 2014, the European Space Agency (ESA) started the Sentinel-1 mission, characterized by a constellation of two polar-orbiting satellites (S1A and S1B), sharing the same orbital plane, which acquires imagery based on C- band with a synthetic aperture radar. The C-band is common in SAR systems and it ranges a frequency from 7.5 GHz to 3.75 GHz and a wavelength from 4 cm to 8 cm [12].

The first satellite, S1A, launched in 2014, has a 12-day orbital repeat cycle and since the second satellite, S1B, has been launched in 2016, a 6-day exact repeat observation has been possible [13]. The high temporal and spatial resolution, of this mission, provide high quality information and allow monitoring of Earth's environments and human activities (e.g. shipping activities). Each Sentinel-1 mission satellite offers different resolution modes (down to 5 m), different coverage range (up to 400 km) and short revisit times (every 12 days).

Sentinel-1 sensor has four operation modes: the Stripmap (SM); the Interferometric Wide Swath (IW); the Extra-Wide Swath (EW); and, finally, the Wave mode (WV). SM, IW and EW modes are available in single (HH or VV) or dual polarization (HH + HV or VV + VH); while WV mode can only be found with a single polarization (HH or VV). Each mode of operation can produce products at SAR Level-0, Level-1 or Level-2 [13].

Level-1 can be provide through Single Look Complex (SLC) products or Ground Range Detected (GRD) products; in the first case, the Level-1 product is geo-referenced using the orbit and the altitude data from the satellite and it conserves the phase information, while, in the second case, it has been detected, multi-looked, and projected to ground range using an Earth ellipsoid model and the phase information is lost. All operation modes can provide the three level products, except for the WV mode which can only offer the Level-2 Ocean (OCN) product [13].

The implementation of the different operational modes depends on the purpose of the analysis and on the respective application. Sentinel-1 applies to different activities, such as the maritime monitoring, which includes ice monitoring (Arctic and sea-ice), ship monitoring, oil pollution from oil spills monitoring and marine winds detection; land monitoring, like forestry, agriculture, urban deformation mapping, flood monitoring, landslide and volcano monitoring and, finally, earthquake analysis. For all these applications, the best suitable acquisition mode is the interferometric wide swath (IW), commonly used for land monitoring. It collects data with a 250 km swath width, from 2.7 x 22 m to 3.5 x 22 m of spatial resolution in the Level-1 SLC product and 20 x 22 m in the full-resolution Level-1 GRD [13]. Therefore, high spatial resolution images can be created. Spatial resolution refers to the size of the pixels in the grid and it provides information about how much the ground surface is covered by a single pixel. High spatial resolution images are very detailed, but they increase the size in the storage, and, therefore, are very difficult to manage. Concerning the wet snow cover mapping, the IW mode with a Level-1 GRD product is the best option because it provides a continuous coverage of the ground while detecting the dielectric properties of targets. The Level-1 GRD product is the most commonly used in cryosphere analysis [11].

3.4. Sentinel Application Platform software and tools :

The Sentinel Application Platform (SNAP) is an open source software made available to the public by the ESA on the Copernicus mission web page.

Processing with SNAP is relatively simple once understood the theory of SAR and got used to the Sentinel missions and their specific features. To assist the learning process, ESAs offers and suggests a series of tutorials, by the way of videos and pdf documents, on the web page https://sentinel.esa.int/web/sentinel/home. Moreover, there is a very large and helpful online community of experts which contributes in answering questions and solving problems.

However, an important aspect of the practical use of SNAP is to not underestimate the sequence of image manipulations. Manipulations employ different tools and their order is dictated by the purpose of the analysis and the type of study carried on, e.g. interferometry, polarimetry or simple pre-processing and geocoding. So, a well knowledge about the methodology is highly recommended before starting the practical phase.

Despite this, the only problem encountered with the software is that requires very powerful computer processor and large memory capacity, which are not always available in the working space. Memory problem is due to the software saves and stocks of new different files after each manipulation, which reduce quickly the available capacity. However, this can be simply overtaken and solved by eliminating manually original and aimless files from the stocking folder. This would significantly reduce the time taking aspect of the analysis.

Nevertheless, difficulties may be found during the image manipulation process due to the size of the file (i.e. big files) and the loss of data which would constraint the analysis, demanding to restart again the process, and this would take extra time during the analysis. Images manipulation with SNAP is time taking and the optimization of procedures, through a model builder, is not always possible due to the loss of data.

3.5. Swiss Data-Cube :

Remote sensing raster images, known also as Earth Observations (EO), can be hard to manipulate and the pre-processing that they require are, often, time taking processes. New innovative technology such as EO Data Cubes (DC) can significantly improve the access to EO data for users by offering large spatio-temporal data, ready to be analysed [14]. In fact, the generation and storage of Analysis Ready Data (ARD) can be very beneficial for users, improving their way to work, minimizing the time and the scientific knowledge required to access the data and avoiding complicated satellite data pre-processing.

EO Data Cubes born in order to overcome satellite raster issues, such as the increasing volumes of data, their storage and the difficulties which processing data generates to the users [14]. They can store different kind of data, generated by different satellites, such as Landsat, MODIS or Sentinel. These new tools work like a database of ARD, which, according to the Committee on Earth Observation Satellites (CEOS), can be defined as processed sentinel data which has been organized in order to be immediately available to be analysed [15]. ARDs need, mainly, metadata and all pre-

processing such as radiometric calibration and geometric calibration [14]. For radar satellites, i.e. Sentinel-1, this would correspond to gamma naught backscatter products.

Developed, implemented and operated by the GRID-Geneva, the Swiss Data Cube (SDC) is the EO Data Cubes for Switzerland. It aims to support Swiss government, policy-makers, decision-makers and the economic development of the country by providing free available, easy to read and analyse, information. Supported by the partnership among the Federal Office for the Environment (FOEN), the United Nations Environment Program (UNEP) and the University of Geneva (UNIGE), the SDC provides knowledge on the environment using high spatial and temporal EO data. Time-series analysis can also be combined with other geo-referenced socio-demographic, economic, and public administration data [16]. The GRID-Geneva is responsible to share knowledge and information, by training University students to use this innovative technology in order to research, report and monitor environment changes through space and time (e.g. monitor forest cover trends [16]) .

4. Literature review :

Environmental monitoring and, in particular, wet snow cover extent (SCE) observation presents a rich literature which employs C-band SAR images [8]–[12], [17]. In fact, C-band is very sensitive and effective due to the high dielectric property of the wet snow and due to the difference in time of transmission and reception, which measures the distance between the target and sensor, it is also possible to give an estimation of the location of the target [5][12] .

The frequency-dependent backscatter of a snowpack is the aggregation of different scattering types: surface and volume scattering [12]. The total backscatter is influenced by the ground interface, by the snow volume, by the air-snow interface and the interaction of all these elements. While dry snow is composed by ice and air, wet snow is a mix of air, ice and liquid water, therefore microwave frequency fails in penetrating the depth of the snowpack and it is backscattered more, giving a different response than dry snow [12].

Several studies focuses on Sentinel missions because this space component of the European Copernicus program suits environment, climate and security analysis; and, they chose Level-1 products from the Interferometric Wide (IW) swath mode [2] [12][18]. Analyses are often local sited and they compare Sentinel results with other images from different satellite missions, such as MODIS or Landsat [2], [18]. However, most researches' methodology is based on the Nagler and Rott's methodology [19]. This methodology employs backscatter values and a soft threshold to separate wet snow from dry snow.

Backscatter signals, such as *sigma naught* σ^0, can determine differences in targets respect to their water content or their surface characteristics. In fact, when the surface is frozen, e.g. dry snow cover, it has a higher scattering albedo intensity and, therefore, the value of the sigma naught will be higher than a moisture surface with more water liquid content [18]. *Sigma* σ^0values decrease with increasing liquid water content and it has a significant variation with the incidence angle, wavelength, and polarisation, as well as with properties of the scattering surface [20].

The backscatter signal strength of a target is often associated to the dimensionless normalized radar cross section or backscattering cross section (σ^0), which is the scattering cross section in the direction toward SAR [5]. The backscatter coefficient σ^0 is used to quantify the power reflectivity of the target and it is the sum of the radar cross sections σ_n of all scatters in an area A, normalized by this area [6]:

$$\sigma^0 = \frac{\Sigma_n \sigma_n}{A} \quad [1]$$

All backscatter coefficients, σ^0 , β^0 and γ^0 are the ratio of the scattered power (*Ps*) over the incident power (*Pi*), normalized by the given area [21]. When the reference area A_β (solid rectangle) is defined to be in the slant range plane, the resulted backscatter will be the *beta naught* β^0 backscatter, or radar brightness [21]:

$$\beta = \frac{Ps}{Pi} \rightarrow \beta^0 = \beta \,/\, A_\beta \quad [2]$$

If the reference area is the ground area, A_σ, then the result is *sigma naught* σ^0 [21]:

$$\sigma^0 = \beta^0 * A_\beta \,/\, A_\sigma, \quad [3]$$

If the reference area is instead defined to be in the plane perpendicular to the line of sight from sensor to an ellipsoidal model of the ground surface *Aγ* (dotted rectangle), then *gamma naught* γ^0 is the result [21]:

$$\gamma^0 = \beta^0 * A_\beta \,/\, A_\gamma, \quad [4]$$

According to Small et al., the *beta naught* β^0 backscatter is the best suitable backscatter because it gives the best estimation of what the radar measures. The σ^0 or γ^0 backscatter values may be terrain-geocoded using a digital height model (DHM), i.e., resampled into a map geometry, producing a geocoded-terrain-corrected (GTC) product, whose radiometry still is ellipsoid-model based [21]. Backscatters σ_E^0, γ_E^0 are geometrically terrain corrected, however, according to Small et al., previous methodologies, concerning conventional ellipsoid earth model or "angular slope correction" using σ^0 normalization with a local incident angle metric, fail to reproduce the topographic variation. In fact, deficiencies created with a geocoding-terrain-correction based on an ellipsoid model will decrease the quality of the backscatter retrieval. For this reason, they should be substituted by radiometrically terrain corrected backscatters, σ_T^0 , γ_T^0 , which integrate terrain variations. The terrain-flattened γ_T^0 normalization convention is converted directly from the beta naught β^0 :

$$\gamma_T^0 = \beta^0 * A_\beta / \int_{DHM} A_\gamma, \quad [5]$$

This '*flattening-gamma'* radiometric terrain correction (RTC) approach, that he suggested, contributes more in suppress a large part of the brightness variation in the SAR images caused by the

terrain variation, avoiding the shadow problem due to topography. In Alpine regions, from hilly to mountainous areas, this is essential because it enables multi-track comparisons of denser temporal sampling rates [2], [11], [21][22].

However, most of the previous study attempt to moderate topography effects by using a local incident angle of the surface and the incidence angle of the satellite, as a proxy for the local area, creating, in this way, more speckles than existed before [2], [10], [12], [18], [19], [23]. They use the digital elevation model (DEM) in order to obtain a local incident angle for the area and apply a geometric terrain correction (GTC) [24].

Once the sampling images have been manipulated, i.e. radiometrically corrected, a comparison among time series images is possible. The use of a reference image, with dry snow cover or bare soil, and images of the snow melting season, with wet snow cover, gives a net distinction between the two categories of snow in heavy vegetated areas. Wet snow cover maps are created by comparing the backscattered values of signals from these coupled images, an image of the melting season and a reference image obtained at snow-free or dry snow conditions [11].

To create wet snow cover maps, ratios of backscattered coefficients or dB-differences are, therefore, used to map the wet SCE in mountain region [9], [10]. Conversion of backscattered ratios or simply of backscattered values to a logarithmic scale (dB) is, thus, necessary, e.g. conversion of sigma naught on dB [13] :

$$\sigma^0(dB) = 10\, log_{10}(\sigma^0) \quad [6]$$

A threshold of -3dB has been commonly used to distinguish the dry and the wet snow cover [2], [8], [21]. When the difference between the signal values of the melting season image and the reference image is lower than -3dB, then, the pixel can be classified as wet snow, e.g. γ^0_Twet – γ^0_Tref [dB]. In open areas, this threshold has been found very effective; however, this -3db threshold may vary depending on the land cover, the rate of vegetation, surface roughness, snow wetness or the radar incidence angle [2], [23].

To overcome the limits created by vegetation, such as in forested environments, a steepness factor can be used to better distinguish the dry and wet snow cover [25]. For instance, a steepness factor of 0.75 can be used to classify pixels as dry snow depending on the altitude.

Otherwise, since the difference between a dry and a wet snowpack can be as low as −1 dB, a softer threshold would provide more information than a -3dB threshold which makes it difficult to detect given the speckle noise in SAR data [2], [12]. Previous researches have investigated over different thresholds in order to find the most accurate one[12]. However, in the mountain regions, the hard threshold of -3dB was revealed effective as in open areas [2].

Results are site located, however the presented methodology to distinguish wet snow cover from dry snow cover has been usually used in the literature as very effective [24].

5. Data and methodology :

5.1. Input data:

Data and images of Sentinel-1 satellite have been collected from the ESA COPERNICUS OPEN ACCESS HUB web site (https://scihub.copernicus.eu/). This Sentinel 1-A dataset of 24 images of Alps were imported into the SNAP software produced by ESA and studied in this analysis.

Images date from January 2019 to June 2019 because, according to Small et al. the springtime melt period in European Alps starts at the beginning of March and ends on June [24]. Images present two different relative orbit numbers, 88 and 66, because they derive from ascending and descending patterns of the S1A platform in the region of the Swiss-Italian Alpes, just underneath Leman lake. Thus, a set of 12 descending (satellite overflight of test area at 05:35.10 UTC) and ascending (overflight of test area at 17:23:23 UTC) images were acquired in both VH and VV polarizations.

Although there is not a significant difference between VV and VH images, VH images have been chosen as the best representable because they generally display a slightly higher probability to detect wet snow cover [2]. The Level-1 GRD products have been collected with the IW mode. The data sets presented are listed in Table 1.

Relative Orbit Number	Orbit	Pass	Polarization	Date	Time
66	25338	D	VV VH	05.01.2019	05:35
88	25360	A	VV VH	06.01.2019	17:23
66	25688	D	VV VH	29.01.2019	05:35
88	25710	A	VV VH	30.01.2019	17:23
66	25863	D	VV VH	10.02.2019	05:35
88	25885	A	VV VH	11.02.2019	17:23
66	26038	D	VV VH	22.02.2019	05:35
88	26060	A	VV VH	23.02.2019	17:23
66	26213	D	VV VH	06.03.2019	05:35
88	26235	A	VV VH	07.03.2019	17:23
66	26388	D	VV VH	18.03.2019	05:35
88	26410	A	VV VH	19.03.2019	17:23
66	26563	D	VV VH	30.03.2019	05:35
88	26585	A	VV VH	31.03.2019	17:23
66	26913	D	VV VH	23.04.2019	05:35
88	26935	A	VV VH	24.04.2019	17:23
66	27088	D	VV VH	05.05.2019	05:35
88	27110	A	VV VH	06.05.2019	17:23
66	27263	D	VV VH	29.05.2019	05:35
88	27460	A	VV VH	30.05.2019	17:23
66	27613	D	VV VH	10.06.2019	05:35
88	27635	A	VV VH	11.06.2019	17:23
66	27788	D	VV VH	22.06.2019	05:35
88	27810	A	VV VH	23.06.2019	17:23

Table 1: Sentinel-1A IW GRD SAR-C products

5.2. Regions of Interest (ROIs) Analysis :

Figure 1: Region of Interest: the Berner Alpen

The study area chosen for this analysis considers the "Berner Alpen", i.e. the Alpine mountain chain among France, Switzerland and Italy. This study observes the mountains nearby the lake area. Distinguishable, from the processed Sentinel-1A images, are the main Swiss larger lakes, namely, the lake Leman (or Geneva lake) and the lake of Neuchâtel close to the smaller lake of Bienne (on its right) and Morat (at its bottom); then, there are the lakes of Thun, Brienz and Lucerne; and finally the big Italian lakes, Maggiore and lake of Como in the middle-right part of the scene, with smaller lakes around them, i.e. lake of Lugano, lake of Varese, Monate, Comabbio and Orta.

5.3. Processing workflow:

As in the previous literature concerning wet snow cover mapping, the methodology employed is the Nagler's methodology [19]. This methodology implies several pre-processing image manipulations to standardize the images. This pre-processing steps within the snow monitoring method are shown in *Figure 2*.

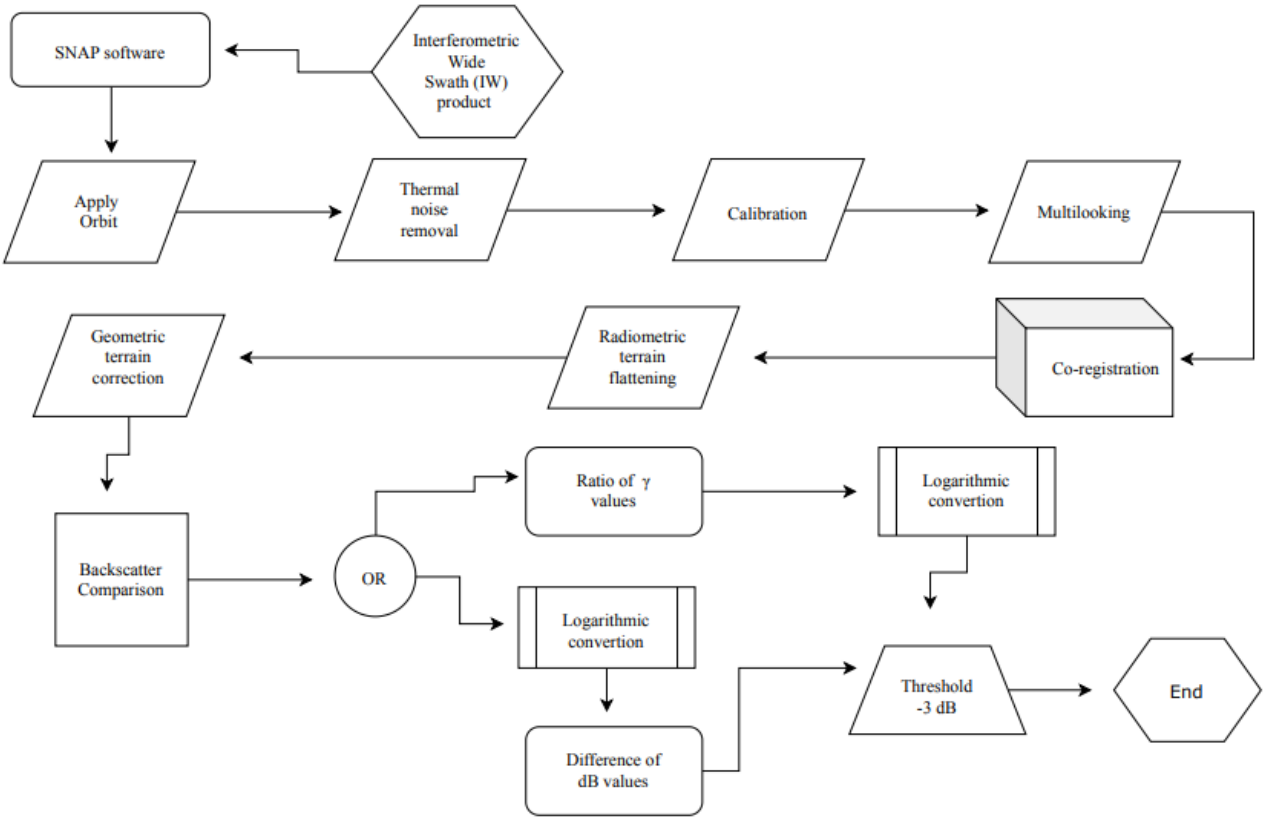

Figure 2: Flowchart of processing steps

5.3.1. Apply Orbit File:

Usually, the precise orbits of satellites are determined and available days-to-weeks after the product to be generated [20]. Therefore, the precise orbit data are, often, not included in many SAR satellite data bundles. Thus, for any future manipulation, it is necessary to acquire and apply first a precise orbit file of the satellite loaded from SNAP's server, which can download and update the orbit state vector (Sentinel Precise – Auto Download) for more accurate information about the satellite position. In this analysis it used a polynomial degree of 3. This process contributes in improving future geocoding and it is mandatory in order to proceed with other manipulations.

5.3.2. Thermal Noise Removal:

The thermal noise removal (TMR) process contributes in normalizing the backscatter signal within the entire Sentinel-1 scene, especially for scenes in multi-swath acquisition modes where it reduces discontinuities in the image intensity values [20]. In GRD images, TNR sets the along range

border stripe values to 1000, which, after calibration, this becomes 0.00225 or -26.4 dB. The TNR have been applied to both polarizations, i.e. VV and VH.

5.3.3. Calibration:

Calibration is the procedure which converts digital pixel values to radiometrically calibrated SAR backscattering, namely sigma, beta and gamma nought. In fact, satellite images are stored in digital numbers (DN) in order to minimize the memory space. Each pixel in the grid provides a single value. A calibration vector, which is included in the Sentinel-1 GRD product, allows the simple conversion of image intensity values into the chosen SAR backscatter. Therefore, the calibration equation is already included into the product, as an annotation [20]. Level-1 products provide four calibration Look Up Tables (LUTs) to produce $ß^0_i$, σ^0_i and γ_i or to return to the Digital Number (DN). The range-dependent gain, applied by the LUTs, includes the absolute calibration constant and, for GRD products, a constant offset is also applied.

5.3.4. Multi-looking:

Multi-looking is the process which generates multi individual looks of the same scene by averaging over range and/or azimuth bandwidths. In fact, in radar terminology, "individual looks are a group of signal samples in a SAR processor that splits the full synthetic aperture into several sub-apertures, each representing an independent look of the identical scene" [13]. By summing all the looks, a resulting image is created. However, this image will be characterized by reduced speckle and degraded spatial resolution. For VV & VH images, multi-looking can be employed to reduce the large processing size of the image.

5.3.5. Co-registration:

A co-registration process will be performed to align the images in a pixel basis. The co-registered images were generated into one stack in order to make ratios of values, comparisons and RGB compositions easier.

5.3.6. Radiometric Terrain Flattening:

Terrain variations affect not only the position of a given point on the Earth's surface, but also the brightness of the radar return [21]. Therefore, in hilly or mountainous terrain, classical equations, which apply a geocoded-terrain correction using a digital height model (DHM) and based on an ellipsoid-model and, which are used to retrieve radar backscatter, are inadequate. Backscatters σ_E^0, γ_E^0, which are geometrically terrain corrected, fails in representing backscattering values in regions where land cover induced backscatter differences, i.e. mountain or hiss regions. Therefore, due to the topography of these regions, comparison of different images or tracs seems to be difficult and challenging. The radiometric terrain-flattening normalization aims to integrate terrain variations, by converting values directly from the beta naught β^0 into radiometrically terrain corrected backscatter, γ_T^0 . This process is necessary in mountain regions because it avoids the issue related to the angular dependence of the backscatter and allows comparison among different images of the same scene.

5.3.7. Geometric Terrain Correction:

Since SAR data are generally sensed with a varying viewing angle, greater than 0 degrees, the resulting images present some distortions related to the side-looking geometry. Terrain corrections are intended to compensate for these distortions [13]. The Range-Doppler Terrain Correction would be applied to all the images to compensate the distortions from the terrain. This type of correction aims to adjust geometric distortions caused by topography, such as foreshortening and shadows, using a digital elevation model to correct the location of each pixel. The Range-Doppler Terrain Correction operator, available in SNAP, implements the Range Doppler orthorectification method for geocoding SAR scenes from images in radar geometry [20]. It uses the available orbit state vector information in the metadata, the radar timing annotations, and the slant to ground range conversion parameters together with the reference digital elevation model data to derive the precise geolocation information [20]. During the geometric terrain correction, raster images can be projected. In this study, images have been projected accorded to the Swiss reference system CH1903 + LV95 which has its centre in Bassel (Suisse MN95, EPSG : 2056). This projected coordinate system provides a local ellipsoid which can better estimate the local surface

5.3.8. Backscatter comparison:

Backscatter comparisons of different images of the same track can be possible by following two different methodologies, namely the multitemporal ratios or the dB differences. The first one, requires a ratio between an image with potential wet snow and the reference image which accounts for a season with dry snow cover or bare soil. Therefore, this ratio can be calculated as follow:

$$Ratio = \frac{\gamma o\ (\text{intensity})}{\gamma \text{referenceo}\ (\text{intensity})} \quad [7]$$

Then, it can be converted in dB values using a logarithmic transformation:

$$Ratio\ (dB) = 10 * log10(\frac{\gamma o\ (\text{intensity})}{\gamma \text{referenceo}\ (\text{intensity})}) \quad [8]$$

And finally, a threshold of -3 dB is applied to generate a first estimate binary snow map, where a pixel with a ratio less than -3 dB was defined as wet snow:

$$Ratio(dB) < -3 \text{ dB} \quad [9]$$

The second methodology is similar, but it is based on the differences between the dB values of the compared images. Firstly, before or after the co-registration process, all the images are converted into dB images by applying the logarithmic transformation of the gamma values (γ_T^0). In the case of gamma nought values, they range from -35 dB to 0 dB. Then, the difference between the two images, i.e. the reference image and the potential wet snow image, is calculated and, if the subtraction is smaller than -3 dB, then, the pixel corresponds to the wet snow cover:

$$\text{Difference } (dB) < -3 \text{ dB} \quad [9]$$

This difference between the backscatter values depends on the kind of snow cover: when there is a snow-free or bare soil, the return backscatter from the scene is higher than when there is a higher water content in the snow pack cover. This is translated in darker pixels on the scene which

corresponds to the wet snow cover. This decreasing in backscattering, detected by the satellite, provides clues of existence of wet snow cover.

Finally, dB images have been converted into Tagged Image File Format (.TIFF) which is the most common raster format and can be analysed with other kind of software like ArcMap, GRASS and QGIS. Once transformed, values are stored in 8 bits, which means TIFF image values range from 0 to 255, e.g. a diachronic colour composite image (RGB) can be created. Conversion in Geotiff images allows a series of analysis with ArcMap, like for example, zonal statistics and conversion in vector layers (i.e. point).

6. Analysis and discussion of results :

6.1. Analysis of the reference images:

Previous studies, which have focused on mountain regions, have noticed that the detection of backscatters is influenced by the steep terrain topography which causes geometrical distortions in the result images and in the backscatter values [19]. In mountain area, the local incidence angles have a significant impact in restraining the surface properties influence. In fact, for co-polarized images, when the incidence angle is greater than 20°, the backscatter of wet snow would significantly decrease, but surface scattering will still be dominant, and this will result in a greater influence from the surface properties. If the wet snow surface is rough, the satellite might not be able to distinguish it from a dry snow or snow-free ground. Despite this, when the incidence angle increases, the influences from surface scattering will decrease and the satellite can better detect the difference between the categories of snow cover. In cross polarization detections, as the study case, backscatters are not significantly influenced by low incidence angles and radar shadows are reduced which gives a further advantage in distinguishing the wet snow cover. The VV and VH images did not show significant distortions or changes related to incidence angles because the incidence angles were relatively high, around 45° which is the most suitable for very wet snow detection with a rough surface.

Following the previous introduced methodology, the raw data detected by the satellite S1-A have been processed, terrain flattened and geocoded. An example of calibrated images can be found in the *Supplementary Information*. Results present a series of images like *Figure 3*.

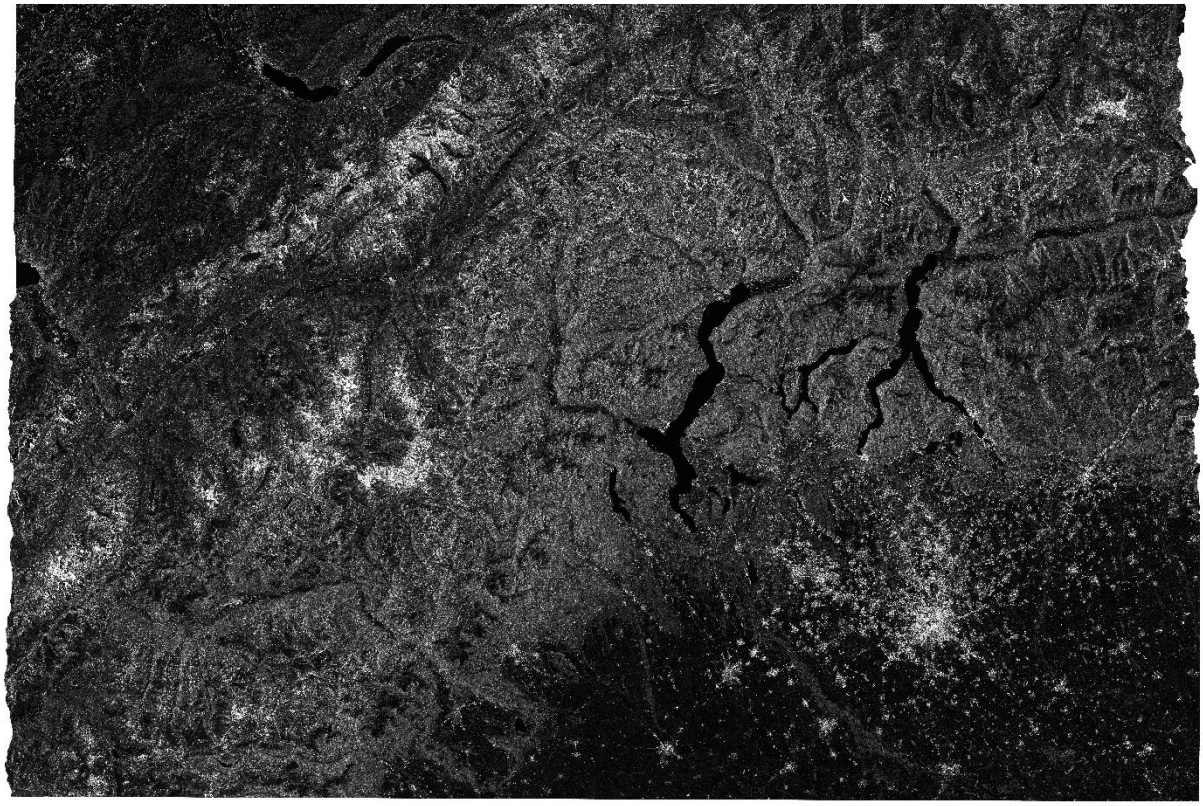

Figure 3: VH image of 5th of January

Despite the flattening process, the mountain area is still distinguishable, with the two big lakes, Maggiore and lake of Como in the middle-right part of the scene and smaller lakes around and between them, i.e. lake of Lugano, lake of Varese, Monate, Comabbio and Orta. Brighter backscatters reveal from cities, bare soil and dry snow cover, while vegetation and targets with high water content are shown by darker pixels, i.e. the lakes and the area around Milan city. *Figure 3* represents the relative orbit scene numbered 66, while *Figure 4* represents the relative orbit scene numbered 88. Both images date January 2019 and are the reference images for the wet snow cover detection and mapping as they present a bare/dry snow ground in the mountain area.

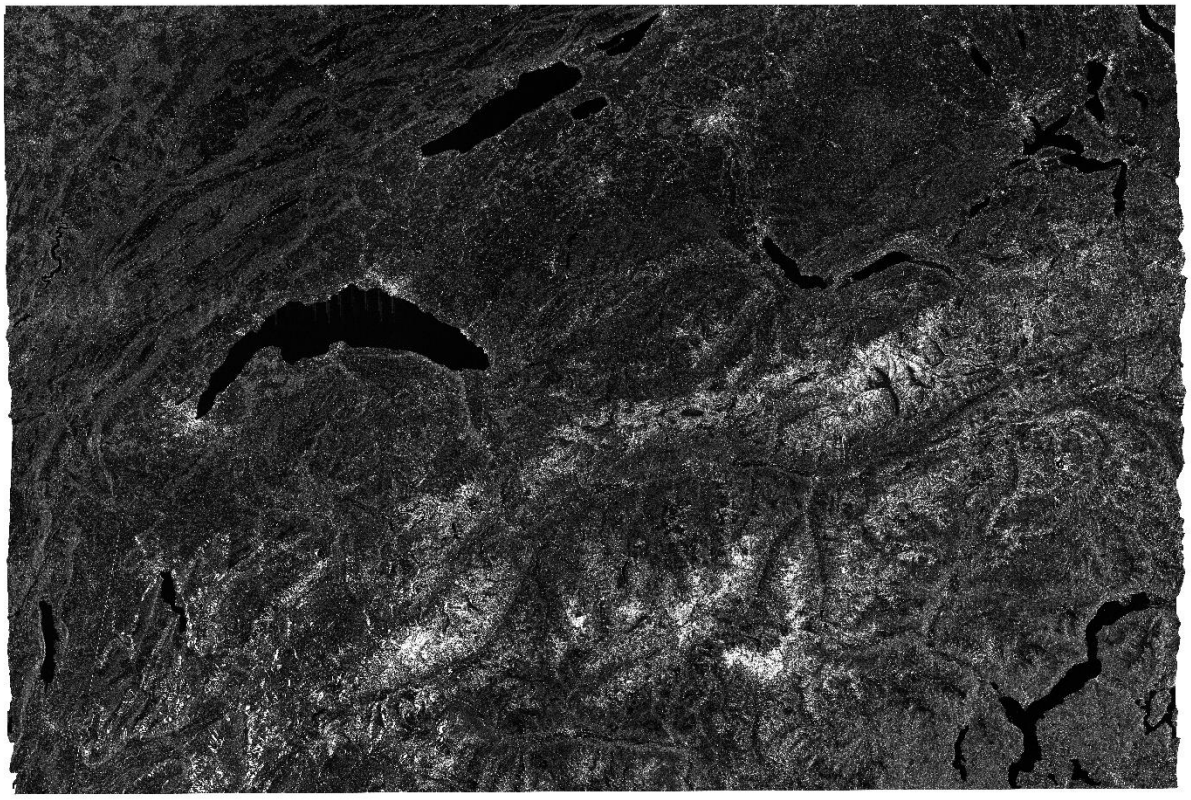

Figure 4: VH image of the 6th of January

Figure 4 presents the lake Leman (Geneva Lake) in the centre-left area of the scene; the smaller lake of Neuchâtel with the lake of Bienne (on its right) and Morat (at its bottom); and, finally, the lakes of Thun, Brienz, Lucerne and Zug in the middle-right part. A small part of the Lake Maggiore reveals in the bottom-right part of the image. In the middle of the scene, appears the Alpine mountain chain, whit brighter pixels. While, closer to the lakes, it is possible to distinguish the city of Geneva, Lausanne; Fribourg and Berne between the lake Morat and the lake of Thun.

The resulting histograms from the backscatter values of the two scenes are presented in the following *Figure 5* and *Figure 6*.

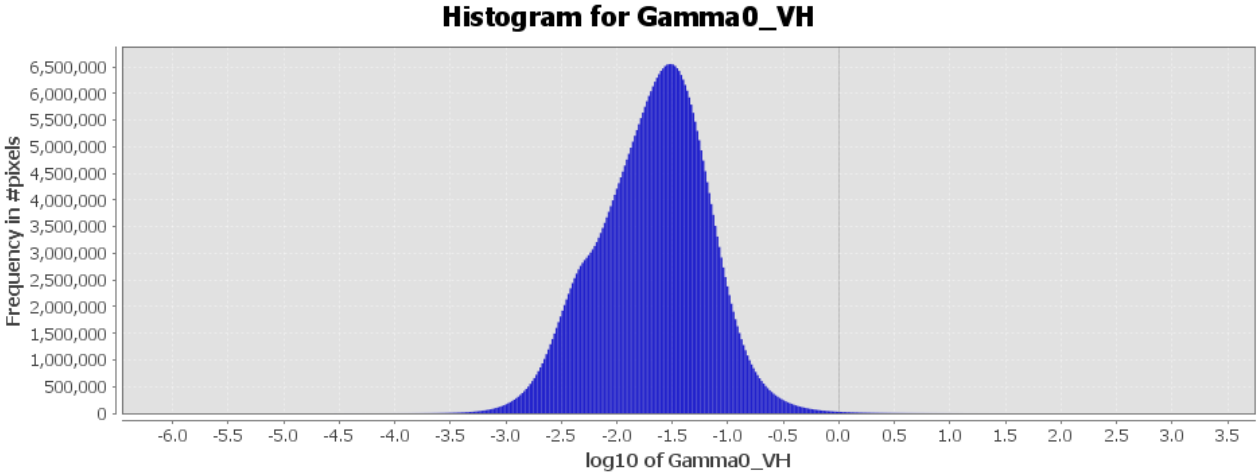

Figure 5: Histogram of the 5th of January VH image (in γ values)

Figure 5 presents the values of the 5th of January VH image in log10 γ values. Data range from -3.0 to 0.0 and the most frequent values range from -2.0 to -1.0 with a significative frequency also from -2.5 to -2.0 (around 3,000,000 pixels).

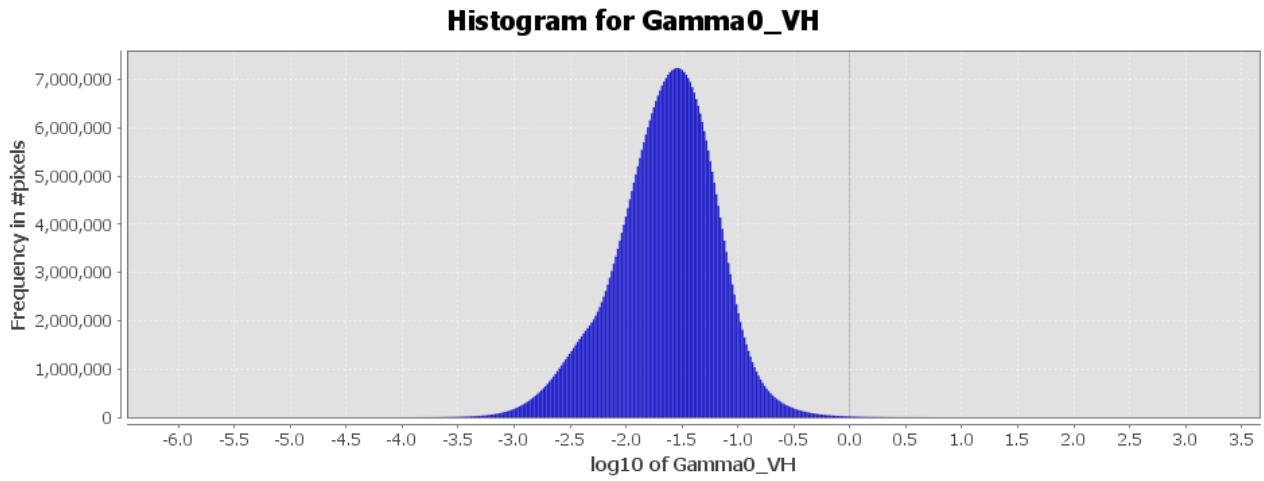

Figure 6: Histogram of the 6th of January VH image (in γ values)

Figure 3 contains brighter pixels than *Figure 4*, and this is also observable from the histogram of the 6th of January, which has a quite normal distribution of the data, with less pixel values between -2.5 and -2.0 (around 1,000,000 pixels less) and more pixels which range -2.0 to -1.0

A mosaic composition has been created with the two ascending and descending scenes. However due to a significant loss in the spatial resolution, this study will present both scenes separately. The mosaic example can be found in the *Supplementary Information*.

6.2. Scene transformation in dB values:

After the image transformations in dB values, the scenes appear brighter. Lakes are more evident, and, even the distinction among the mountains, the city and the nearby area is clearer.

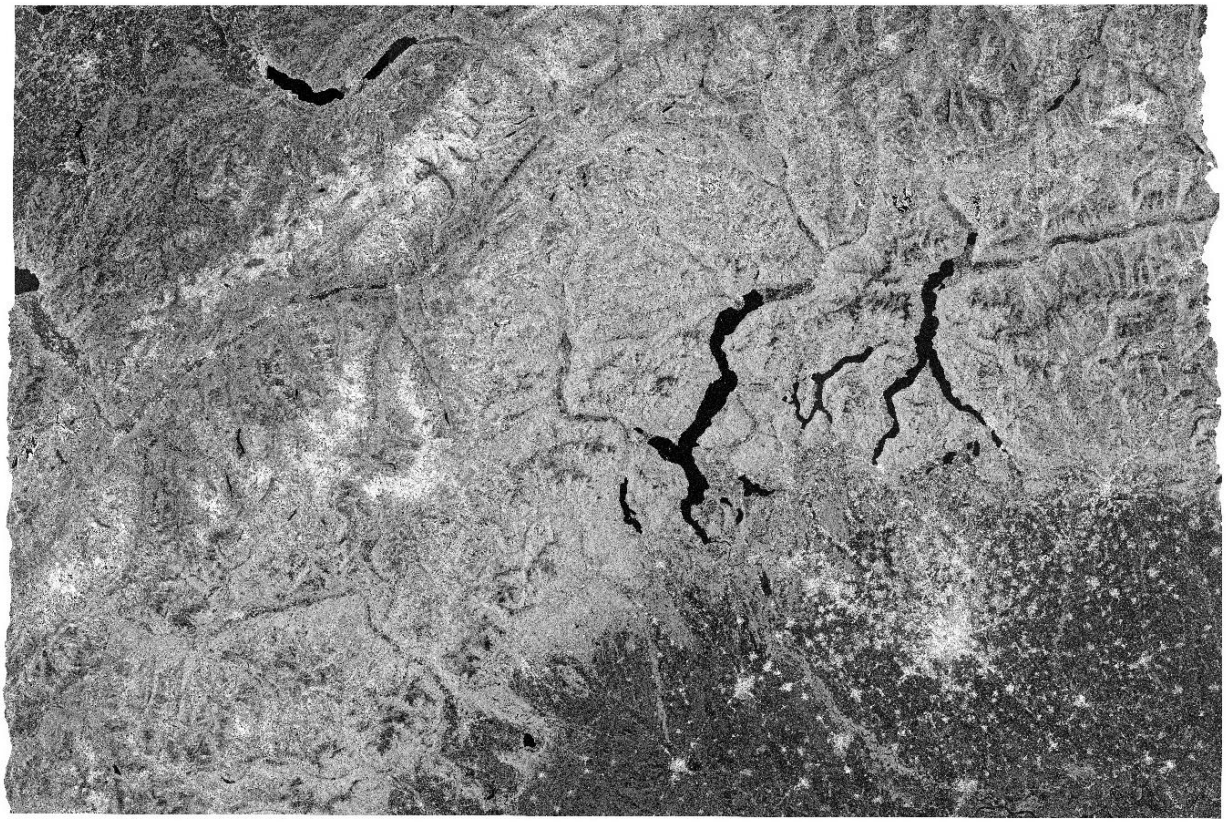

Figure 7: VH image of the 5th of January in dB values

Figure 8: VH image of the 6th of January in dB values

Figure 7 and *Figure 8* show the 5th and 6th of January VH images in dB values. Cities and mountains with dry snow or snow-free soil are completely white, while the rest of the soil in the scene appears in grades of grey and the lakes in black. It is also possible to notice an interference in the radar detection nearby the lake Leman, resulting in white lines over the lake.

The relative histogram, presented in Figure 8, shows the transformation of the image values into dB values which range from -35 dB to -0 dB. The shapes of the two image histograms remain the same but the frequency of pixels is higher, reaching 8,000,000 and 9,000,000 pixels in the respective *Figure 9* and *Figure 10*.

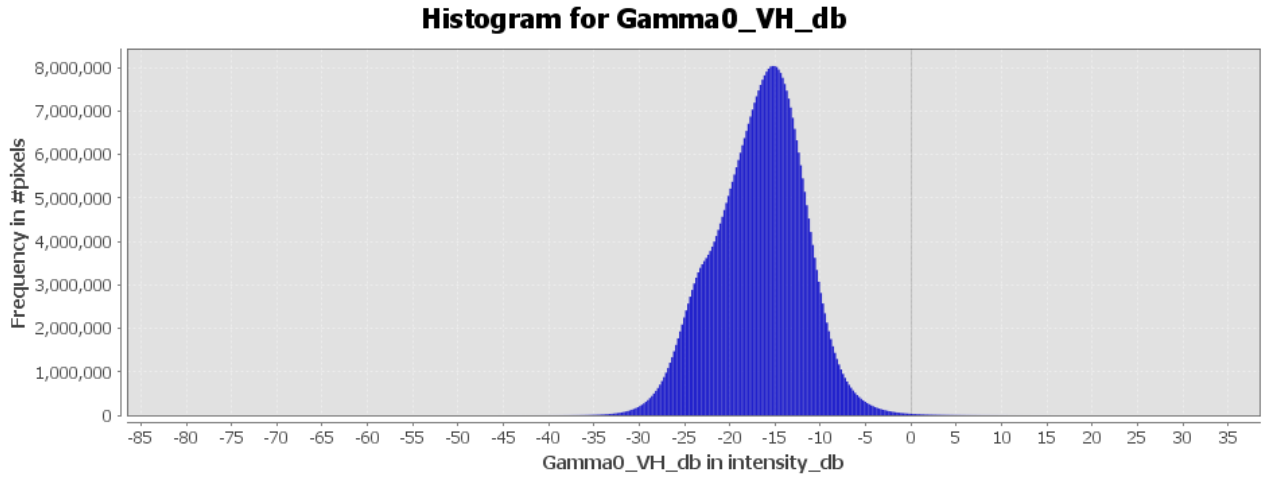

Figure 9: Histogram of the 5th of January VH image in dB values

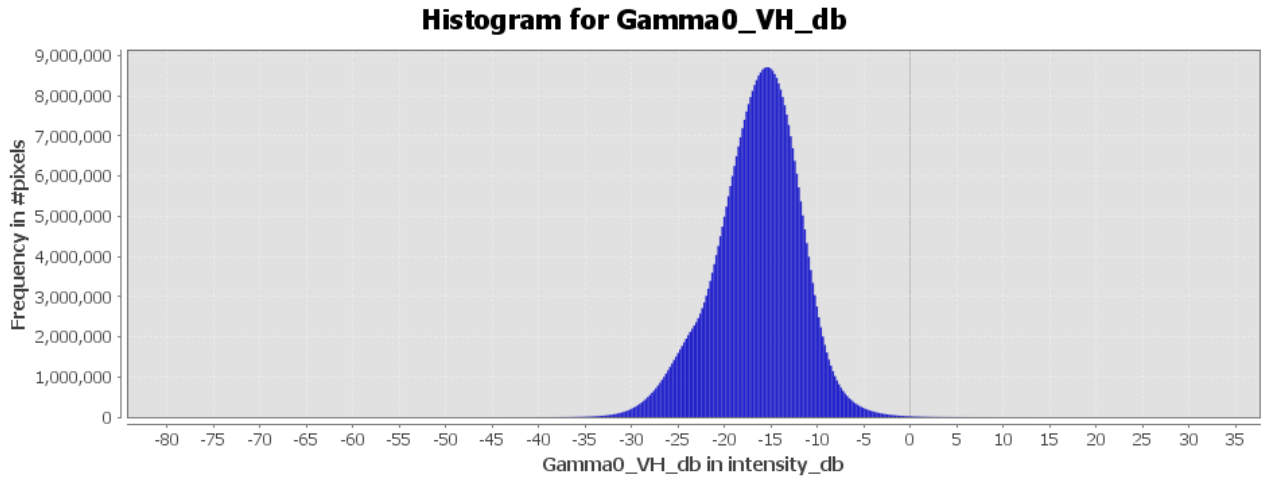

Figure 10: Histogram of the 6th of January VH image in dB values

6.3. Temporal and spatial backscattering comparison:

Histograms are good representations of pixel value changes in time, due to the melt process of the dry snow in wet snow cover. In fact, the following histograms presents different period of the year 2019, starting with the reference images, 5th and 6th of January (respective histograms in *Figure 9* and *Figure 10*), until June 2019.

Starting with the comparison of the images detected on the relative orbit numbered 66, the following histograms date the 30th of March, the 29th of May and the 22nd of June (in 2019).

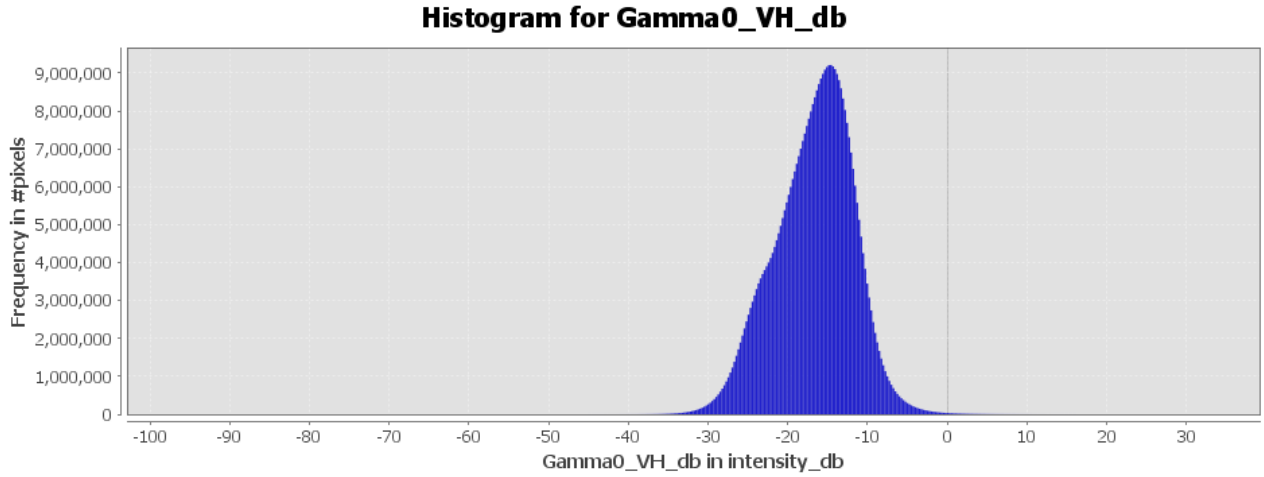

Figure 11: Histogram of the 30th of March VH image in dB values

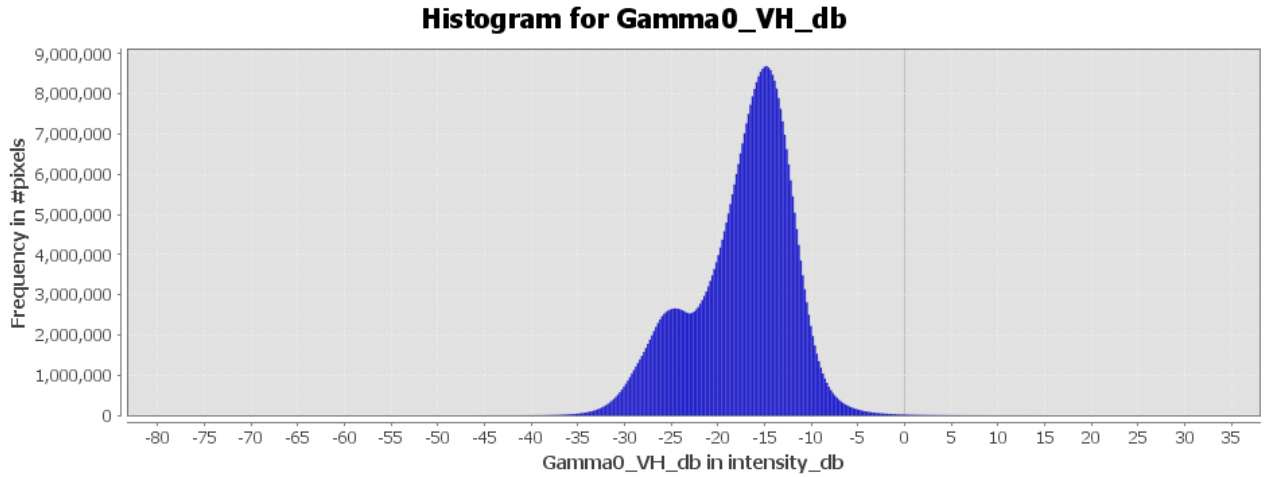

Figure 12: Histogram of the 29th of May VH image in dB values

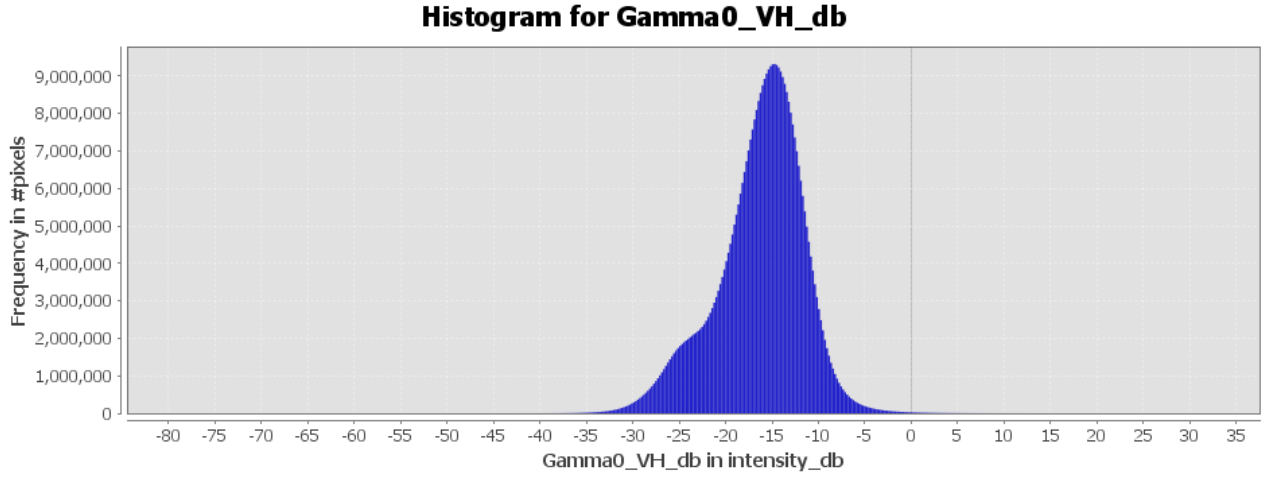

Figure 13: Histogram of the 22nd of June VH image in dB values

From the previous histograms is possible to notice a significant difference in pixel dB values. March season does not present great differences with January because the melting season has not started yet. While, there is a great change between March and May, which presents (this last one) a lesser steep and normal distribution, with more pixel values ranged from -30 dB to -27 dB, creating a wave in the histogram. This change supposes that pixels with dry snow cover, until March, have melted starting from April and the additional water content result in pixels with decreasing dB values which range from -30 dB to -20 dB. This increase in water content detection decreases rapidly within a month, from May to June, and the histogram restores a shape like the original one, with the exception that dry snow cover, after melting in wet snow cover, has disappeared, resulting in bare soil.

Similar outcomes result from the relative orbit numbered 88. Histograms date the 31st of March, the 30th of May and the 23rd of June 2019.

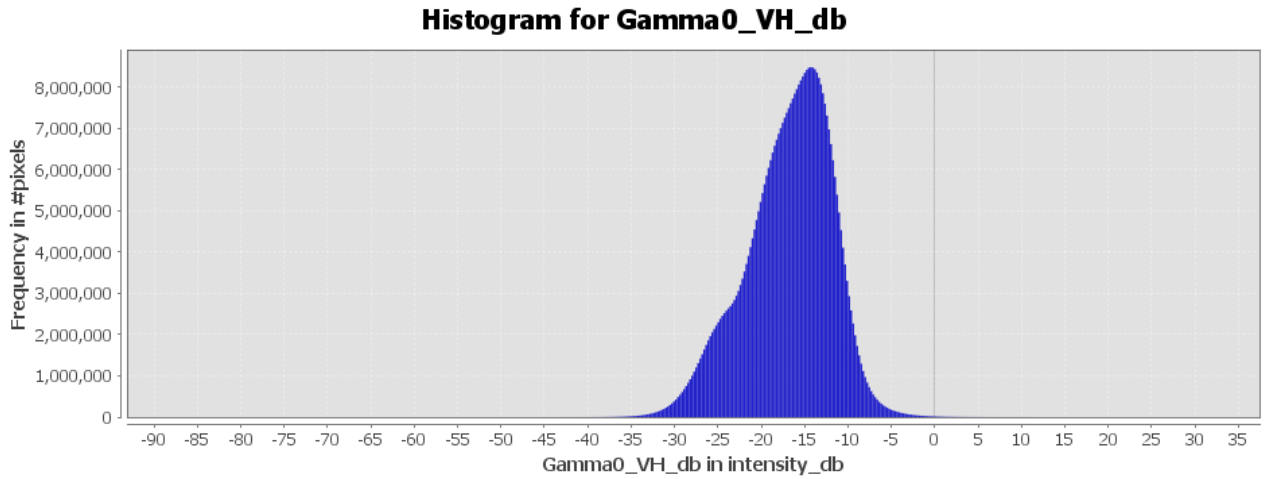

Figure 14: Histogram of the 31rst of March VH image in dB values

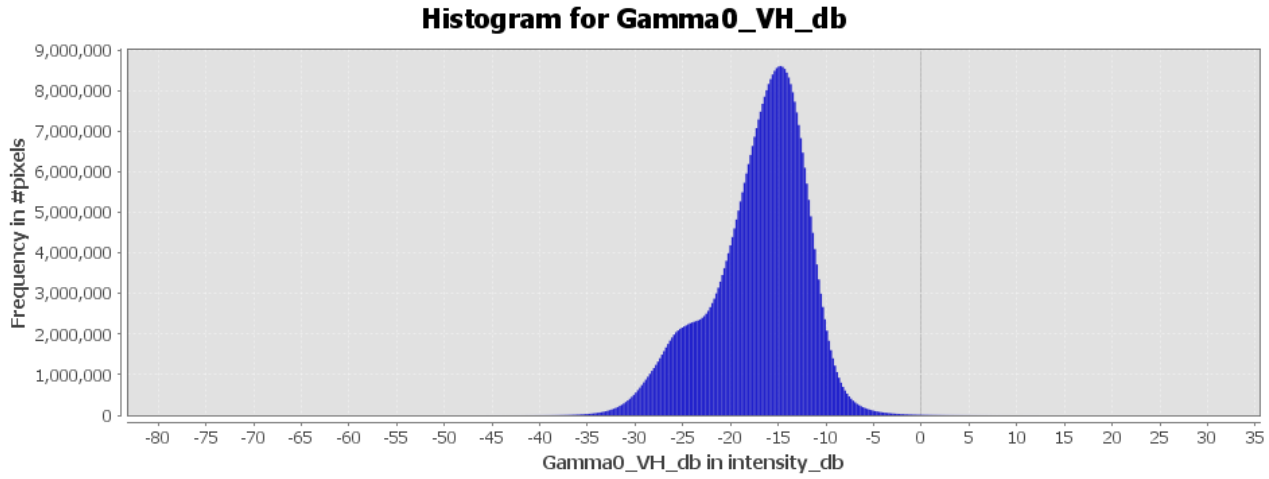

Figure 15: Histogram of the 30th of May VH image in dB values

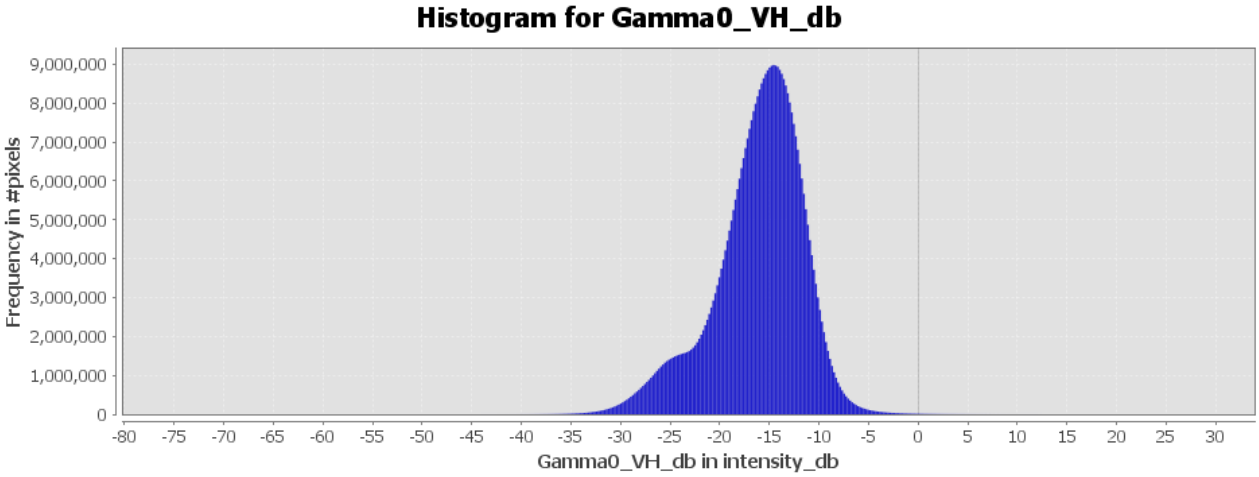

Figure 16: Histogram of the 23rd of June VH image in dB values

From a spatial point of view, changes in backscatter values is observable in the dB images of the relative scenes for the respective months, March, May and June, presented in the following *Figure 17* and *Figure 18*.

a)

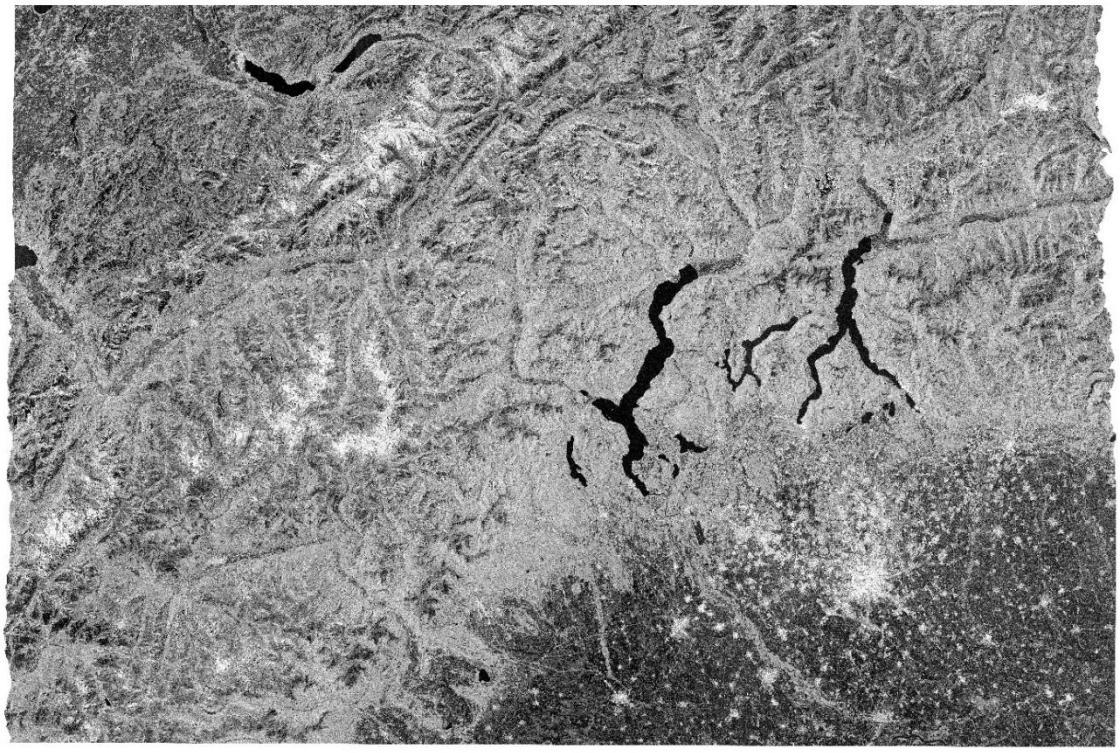

b)

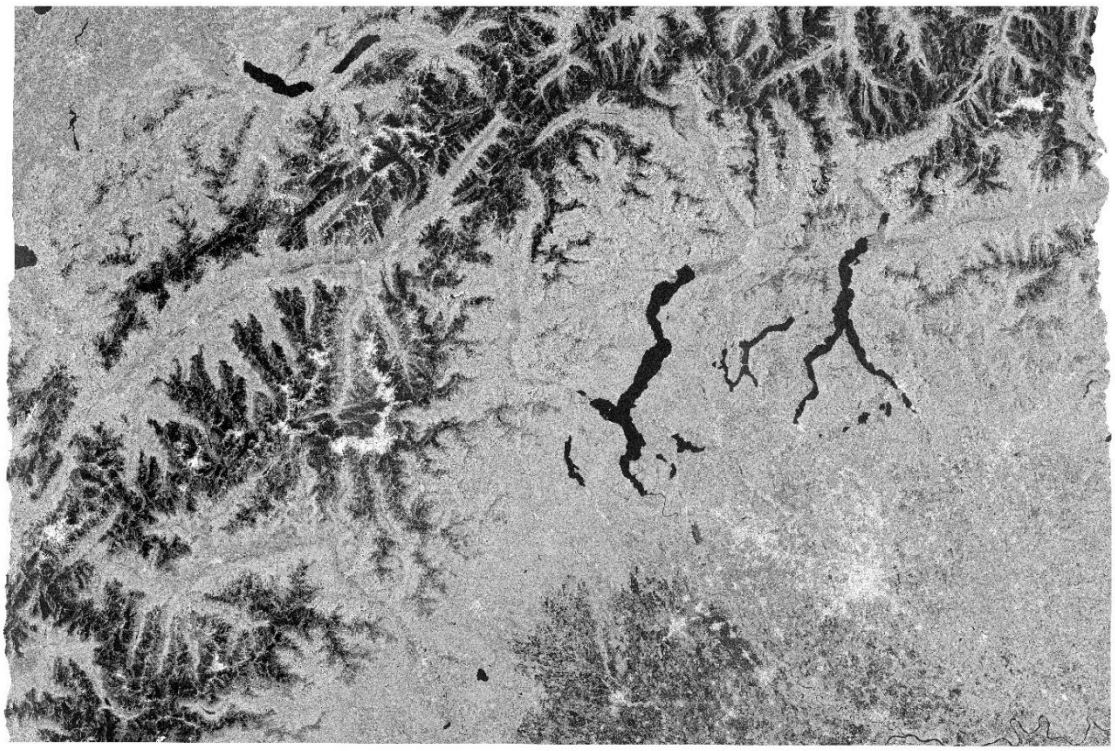

c)

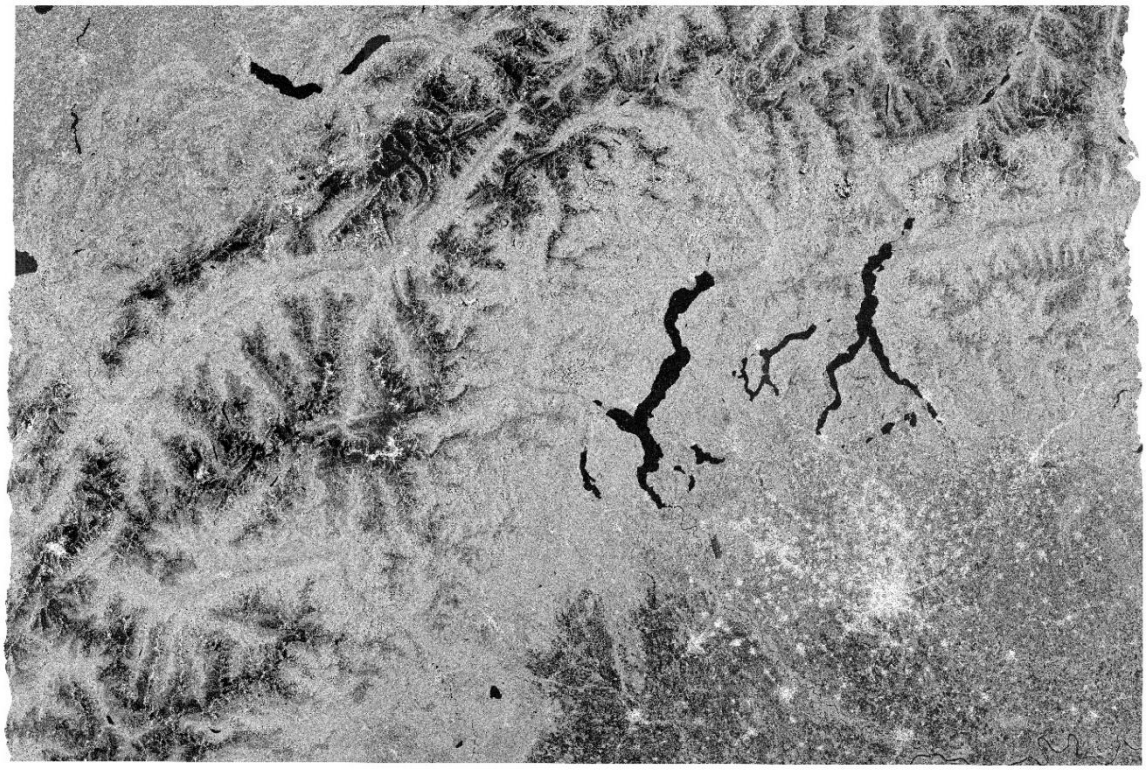

Figure 17: Time comparison of the wet snow cover in dB images. From the top, a) 30th of March, b) 29th of May and c) 22nd of June

The time comparison of the same scene allows to observe the changes in the backscatters and their spatial distribution. In fact, from January to March, there are already slight changes in the backscatters of the mountain surface, which determine the melting season beginning. From March to May, it is possible to observe the melting process of the dry snow cover all along the Alpine mountain chain. Pixels, which were in shades of grey, become darker and even the white pixels in the March

image, which represent the permanent dry snow cover, are reduced in the May and June image, confirming that there is still permanent snow cover on the top of the mountains but there is a reduction due to temperatures and the melting process.

Darker pixels in the image represent the distribution of low backscatters which are the result of increasing liquid water content in the snow pack. Changes in the backscatters appears due to the presence of liquid water and the dielectric contrast between the snow and air boundary. Thus, the surface scattering from the air and the wet snow layer and the volume scattering of the snow pack, contribute together in the backscatter of the wet snow cover. While, instead, seasonal dry snowpack is generally transparent to the C-band SAR observations, so the backscatter values are elevated, and pixels are bright, similar to bare soil. From May to June, it is possible to observe a drying and evaporation process which reduced the water content of the soil and completely melt the snow on the top of the mountains (few white areas in May becomes black in June), which is translated in fewer darker pixels on the overall image respect to the one of May. Another temporal and spatial change reveals from the soil or vegetation around the city of Milan: vegetation/soil has more water content during spring (March) than in summer period (May and June).

Same results are observable from the relative orbit numbered 88 scene. From January to March we observe a slight change in the colour of the pixels, and from March to May, those pixels become completely darker respect to the entire scene. Then, from May to June we observe a decrease in the dark pixels which suggest wet snow cover has been reduced by warmer temperatures and evaporation; and on the top of the mountains pixels becomes completely dark.

a)

b)

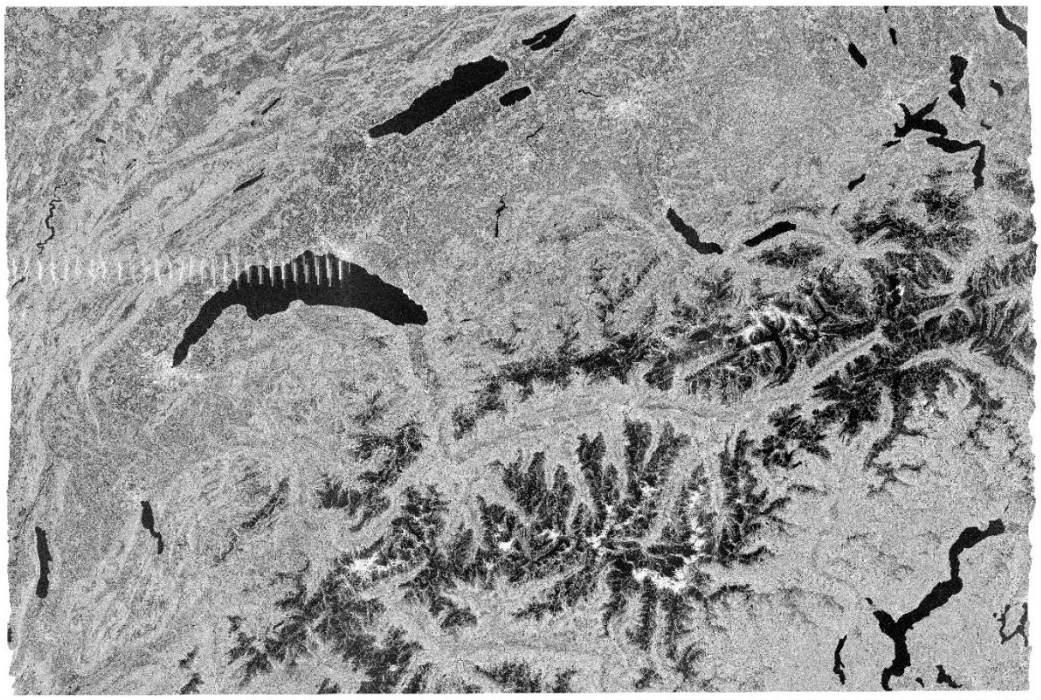

c)

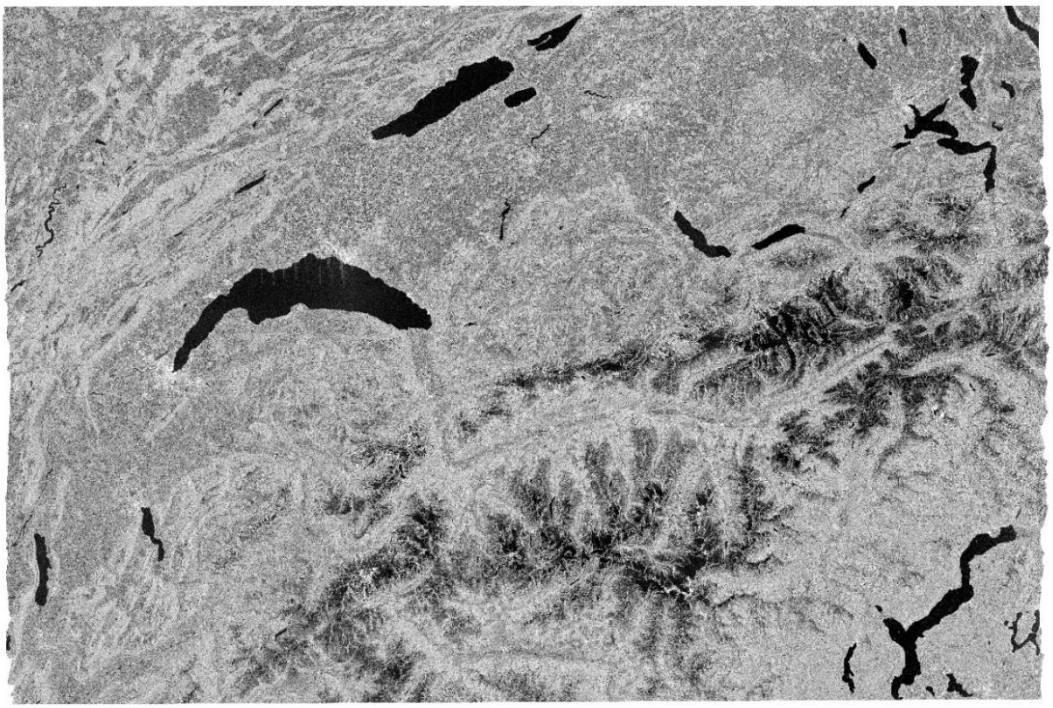

Figure 18: Time comparison of the wet snow cover in dB images. From the top, a) 31rst of March, b) 30th of May and c) 23rd of June

According to the Additive Colour Synthesis, colours are created by mixing three primary colours of light: red, green and blue (RGB). In the following paragraph, a diachronic colour composite image RGB will be presented for both scenes. A diachronic RGB combines different bands acquired at different time for the same scene. Each band is associated to one of the three primary colours of light. The first one, *Figure 19*, for the relative orbit number 66, and the second one, *Figure 20*, for the relative orbit number 88.

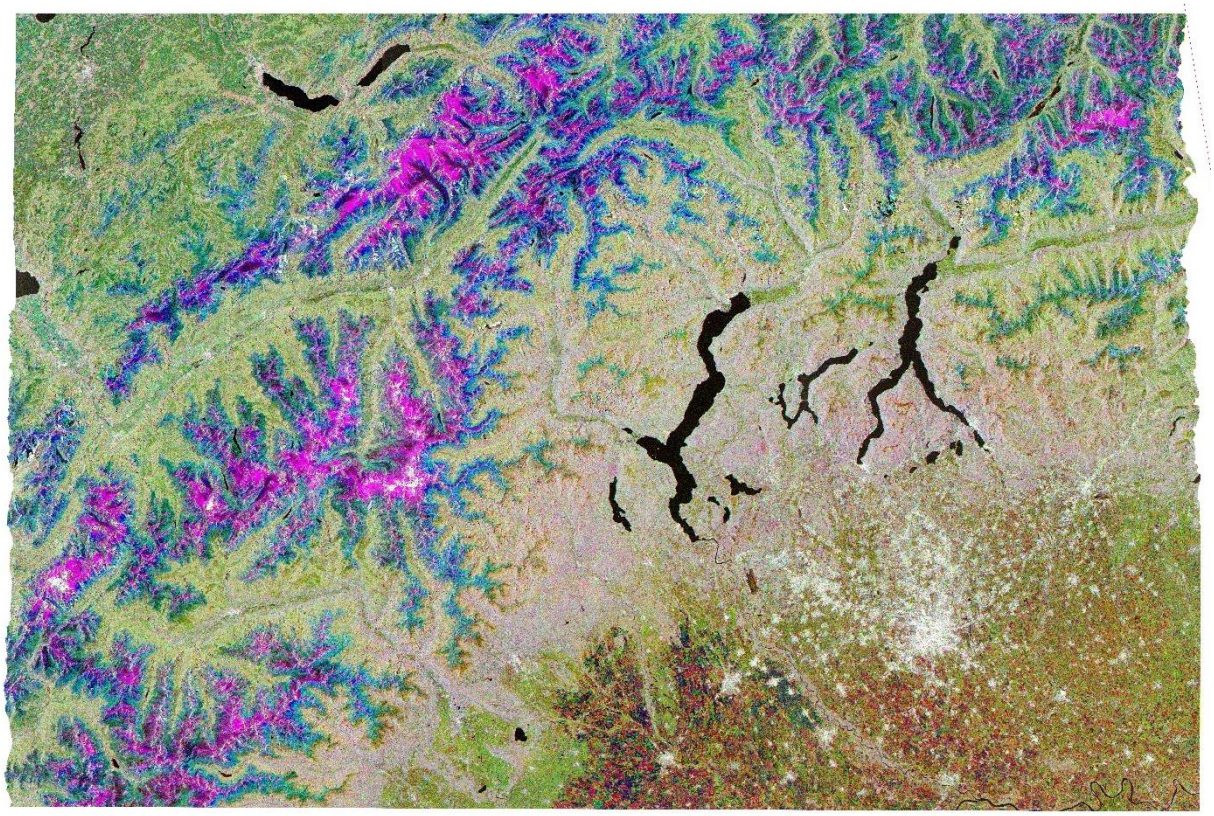

Figure 19: RGB of dB images of January (5th) - April (22nd) - June (22nd)

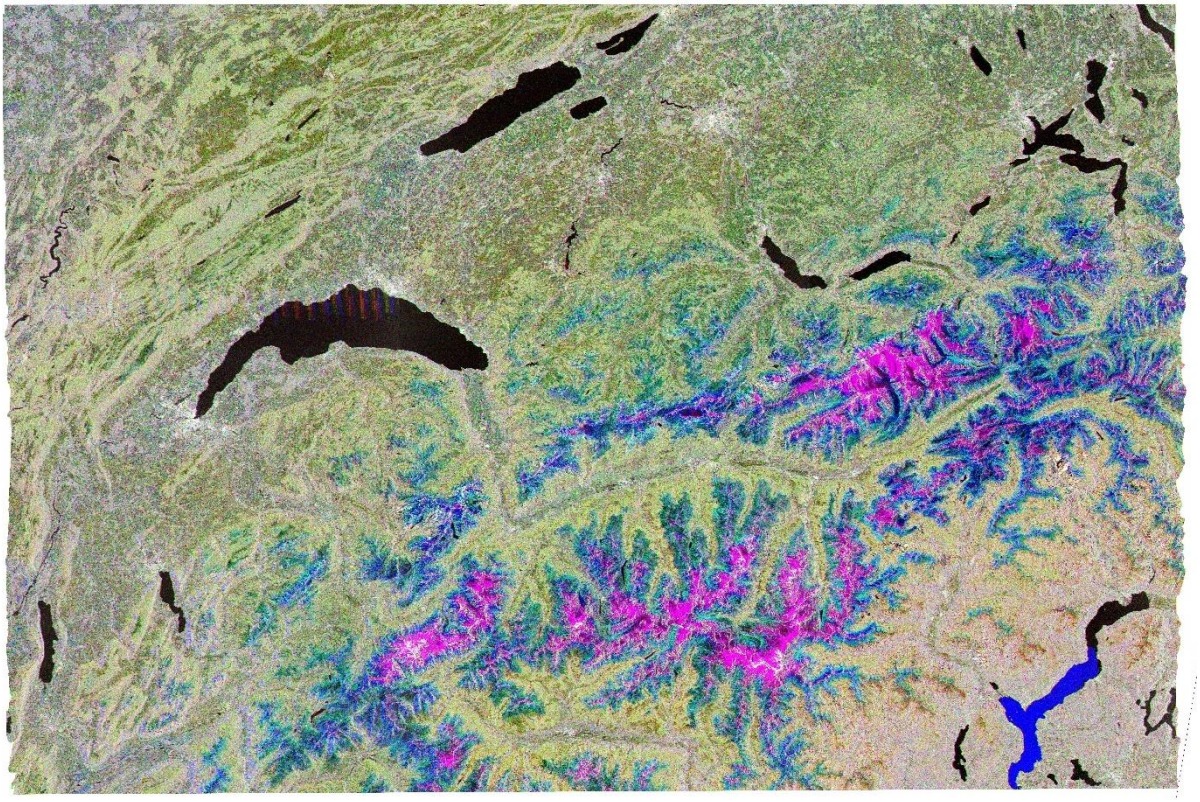

Figure 20: RGB of dB images of January (6th) -April (24th) - June (23rd)

This thematic comparison between seasonal differences in the wet snow cover is represented with a diachronic RGB composition where each colour band has been assigned to a period of the year

studied: in order to exalt the backscatter differences among the moths, the red colour has been associated with April when the backscatter values are lower and there is an increasing in darker pixels; the green band with June where dark pixels of wet snow cover are in small quantities and the blue colour to January 2019 where the dark pixels are at the lower quantity. Variations in the overlay colours represent spatial and temporal changes in backscattering values in the study area. In magenta and cyan are represented the backscatter variations during the study period. Images are in 8bit and values range from 0 to 255.

Also, the graphs of the RGB composites, in *Figure 21* and *Figure 22*, show the changes in the pixels values in the scenes and confirm that this comparative method allows to better identify changes through months.

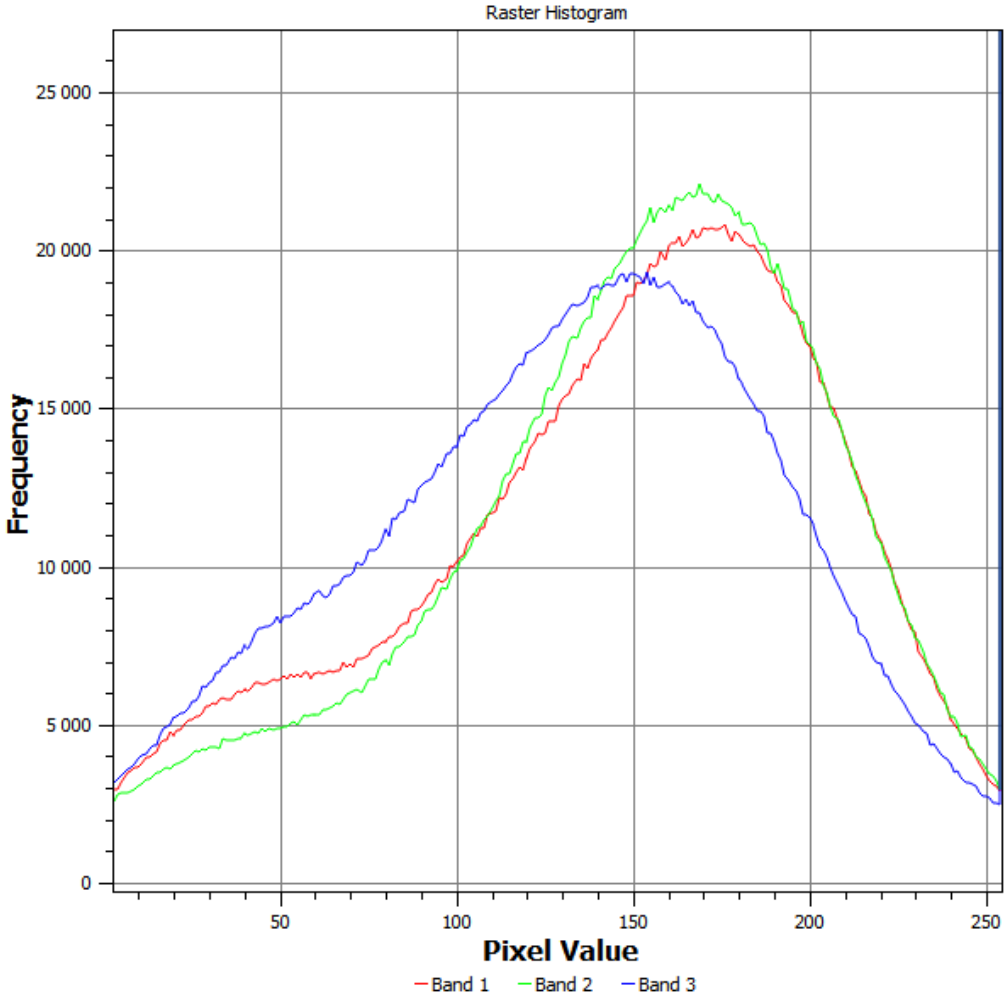

Figure 21: Graph of the RGB (23rd of April in red- 22nd of June in green – 29th of January in blue)

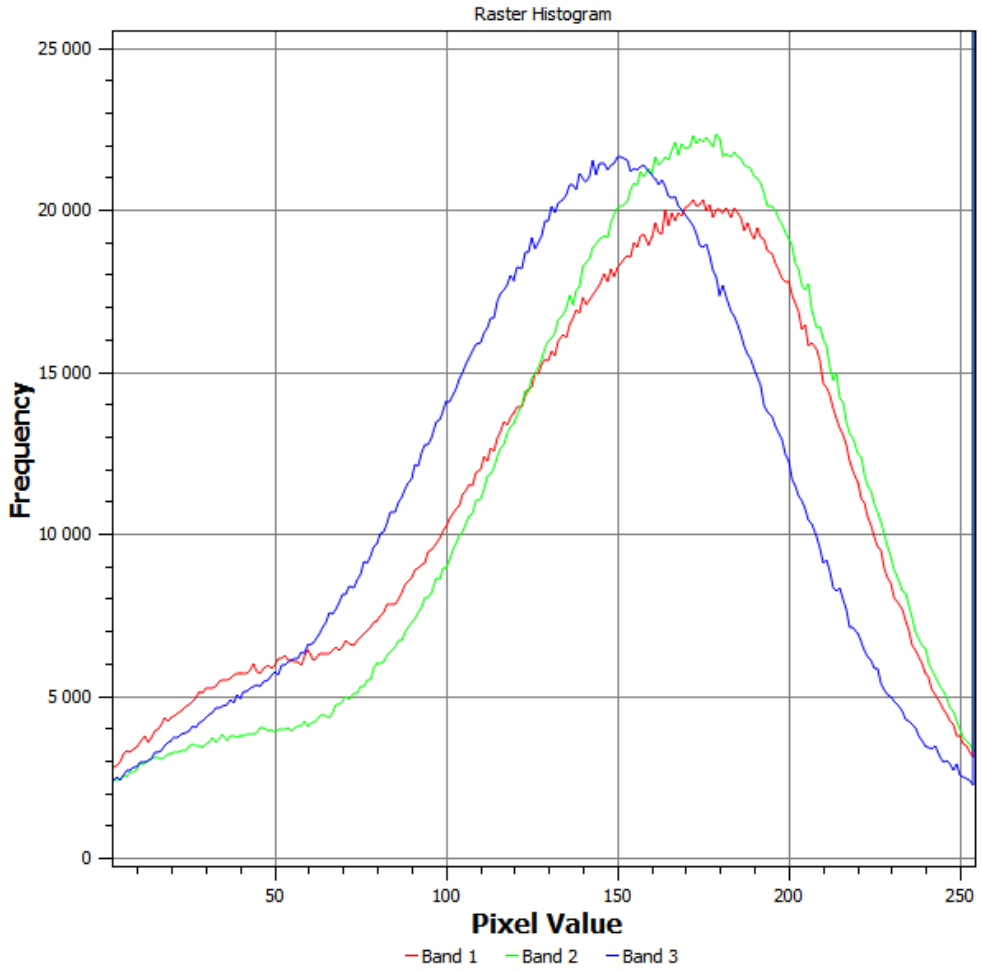

Figure 22: Graph of the RGB (24th of April in red – 23rd of June in green – 30th of January in blue)

6.4. Binary wet snow cover map:

Then, the binary wet snow maps were generated for polarization, applying the -3dB threshold on the resulting image from the difference among the images in dB values. Four representative images have been chosen to present the differences among the images in dB values and are included in the *Supplementary Information*. While the resulting binary wet snow maps, for both scenes, are presented below in *Figure 23* and *Figure 24.*

a)

b)

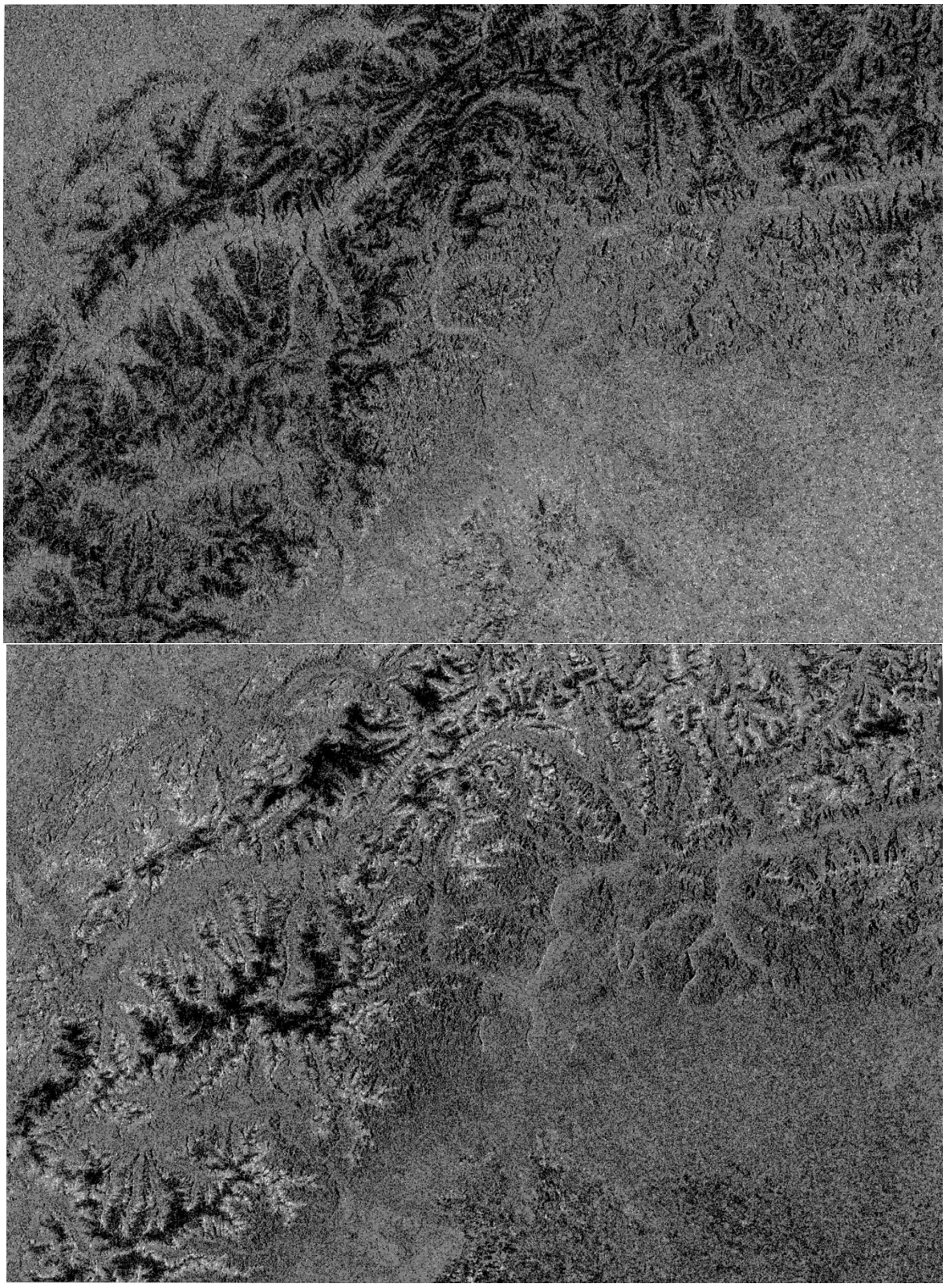

Figure 23: Binary wet snow map of relative orbit scene numbered 66. In withe is presented the potential wet snow cover at the end of April (a) and on June (b)

a)

b)

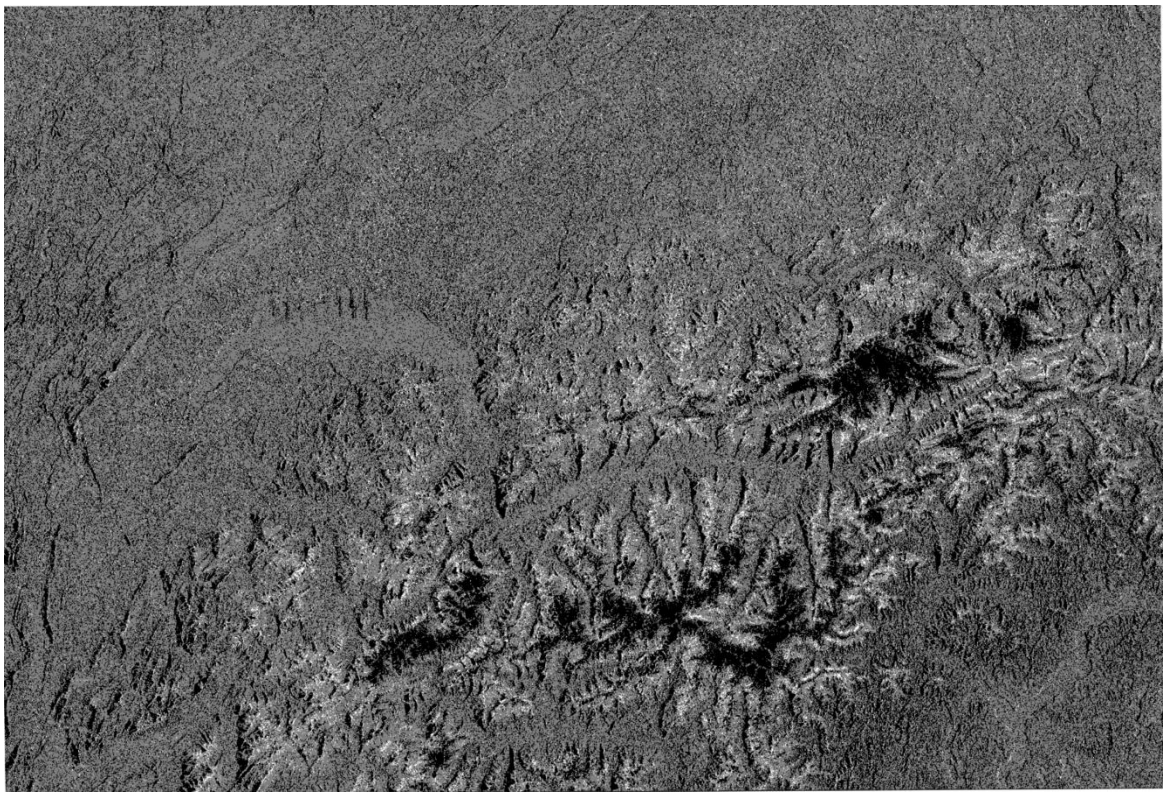

Figure 24: Binary wet snow map of relative orbit scene numbered 88. In withe is presented the potential wet snow cover at the end of April (a) and on June (b)

From the binary snow maps, we observe the potential wet snow distributed in the Alpine mountain region. Wet snow cover is presented in black pixels in both *Figure 23* and *Figure 24*, respectively on late April (a) and on June (b). We can see a significant increasing in wet snow cover

in the springtime with a decreasing during summer, where the wet snow cover appears only on some part of the mountain chain.

Examples of histograms can be seen in *Figure 25* where values inferior or equal to -3 dB are presented in black and other values in grey or white.

a)

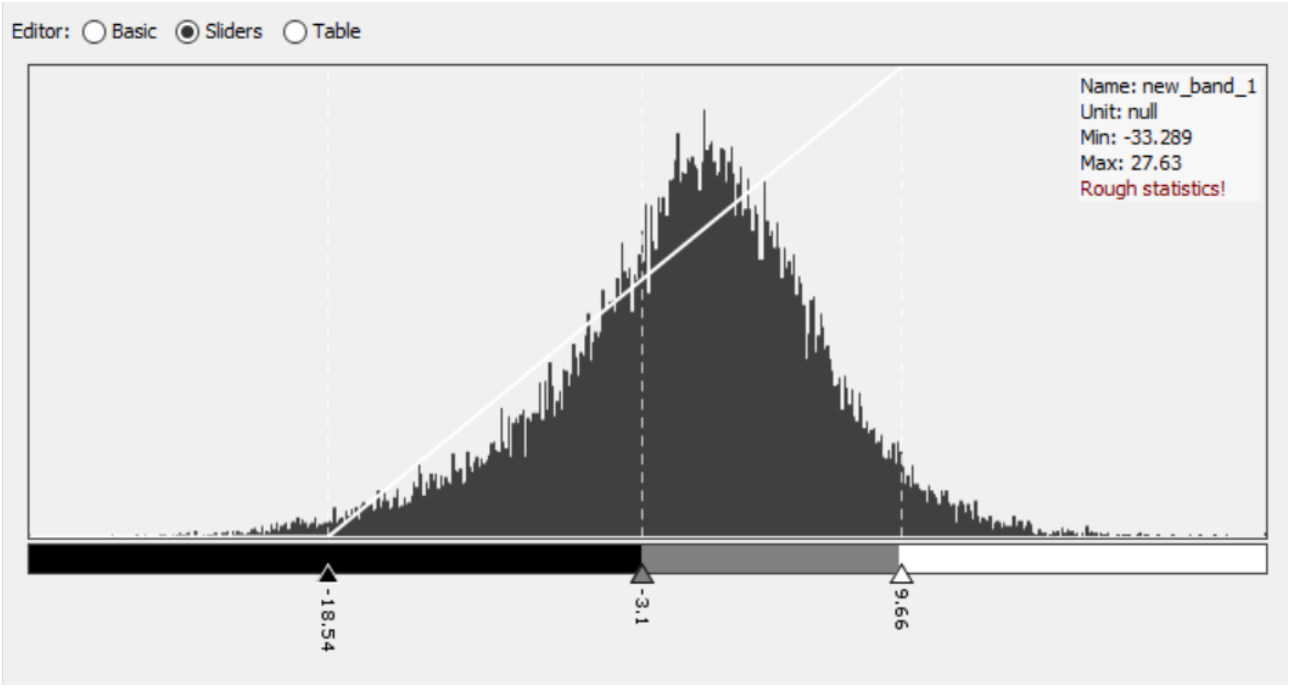

b)

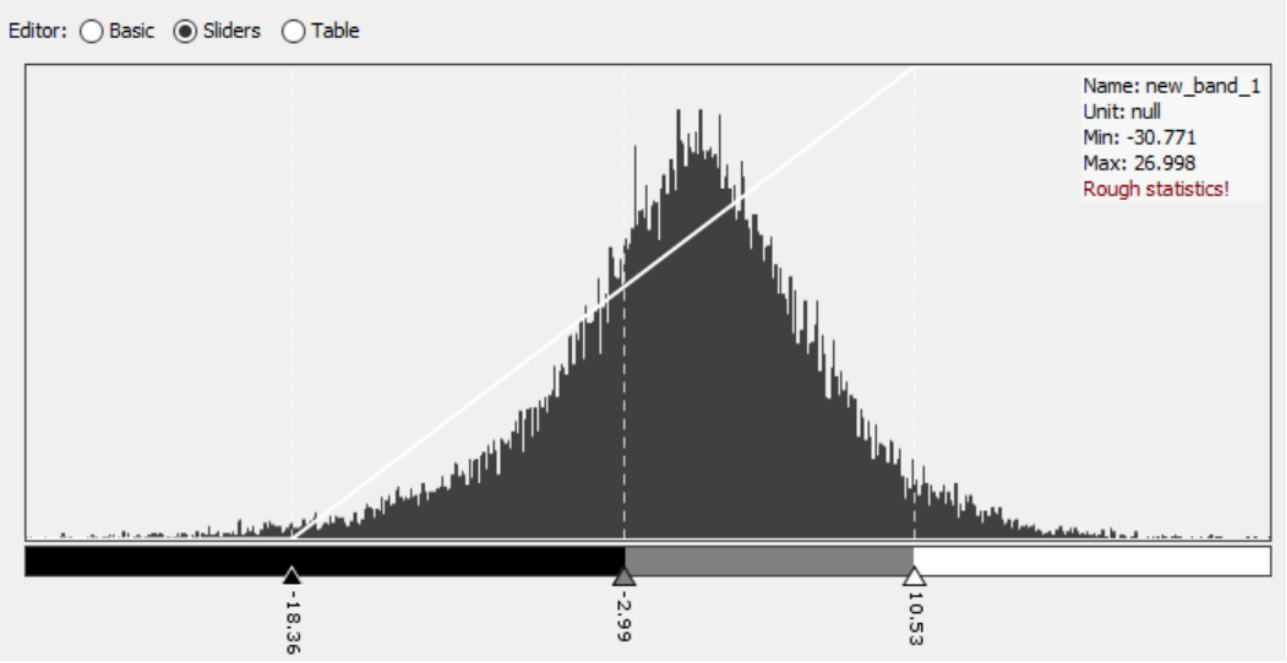

Figure 25: representative histograms for binary maps of the relative orbit numbered 88. a) histograms of wet snow cover appeared from January to April, b) histogram of wet snow cover resulting from April to June 2019.

From *Figure 25*, it is possible to see the difference in terms of number of black pixels in the raster. In fact, this reduction in darker pixels can also be confirmed by a statistical analysis. Once converted into TIFF raster files, wet snow cover pixels have been selected with the Arctool "Raster Calculator" by selecting pixels with values equal to 0. Then, a zonal statistical analysis has been

done and exported in text file (.txt). This process allows results to be analysed with software like Excel, Rstudio, PyCharm or Jupyter Notebook. An example is given by *Figure 26* which presents a simple graph made with Excel. This graph represents the number of wet snow cover pixels in the binary maps, *Figure 23* and *Figure 24*. As it can be observed, these two scenes (i.e. relative orbit numbered 66 and relative orbit numbered 88) presents differences in terms of number of dark pixels in the a) binary map (from January to April), while are quite similar in the b) binary map (from April to June 2019). However, in both relative orbit scene, we observe a decreasing in darker pixels from about 150'000 to 9'000 pixels.

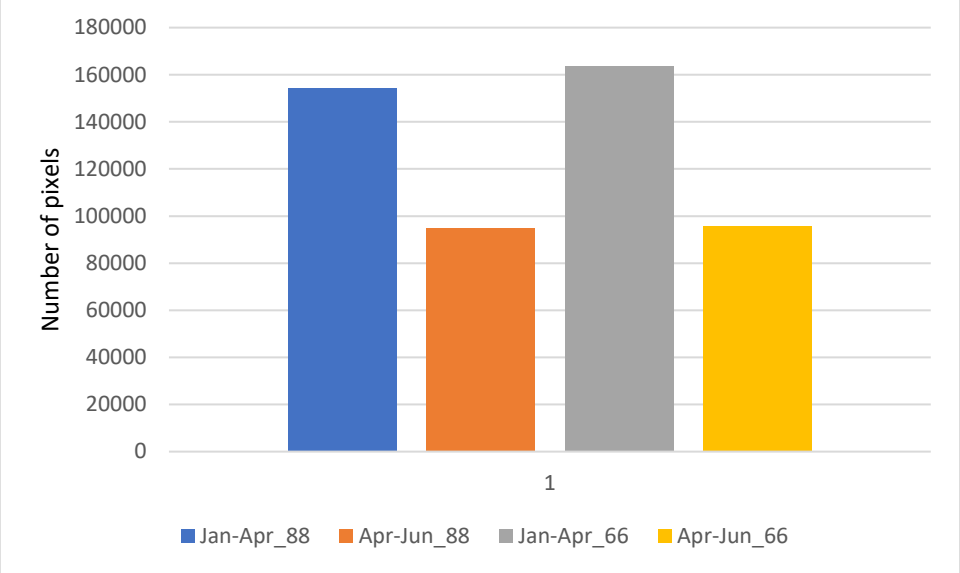

Figure 26: example of graph created with the statistical data extracted with ArcMap. Each column represents the number of dark pixels in the binary maps, Figure 23 and Figure 24 (section a) and b)).

6.5. Uncertainties:

Throughout this study, C-band SAR remote detection with the satellite S1-A has been demonstrated to be capable to detect wet snow cover in mountain regions. In fact, the Sentinel-1 missions provide high instrument stability and the high space resolution with the IW mode. However, due to technical limits, improvements can be made by integrating other form of data and analysis.

First, an average image for the dry snow season (i.e. winter time) can be used as the reference image. In fact, the expansion of the dataset with more suitable images without wet snow cover can provide more general backscatter features.

Second, a good strategy would be to combine remote sensing results with field work datasets, obtained *in situ*, such as more parameters of snow properties, e.g. temperature, depth and wetness. The change detection method is robust to identifying wet snow with decreased backscatter, however, the only threshold cannot classify all the wet snow by the simple linear boundary. The satellite is performant in detecting the changes in the surface due to increasing and decreasing of water content, but it presents limits in distinguish the bare ground to the dry snow pack and therefore, to classify wet soil with wet snow cover. Meteorological data can also be integrated to improve the comparative analysis.

Then, a better kind of soil and land cover classification would need more information about surface roughness which can also be collected from field work, in order to provide more valid support for the analysis of backscatter behaviours. The classification analysis can be improved not only with field work datasets but also through comparisons with other satellite mission datasets, i.e. Sentinel-2, Landsat missions. Once a land cover classification is applied to distinguish snow cover from the ground or water basins, i.e. lakes, the wet snow cover analysis with SAR would be more accurate.

Finally, although Sentinel-1 missions offer a quality information, thanks to the repeat observations of the same scene over time, lack of accuracy and accessibility of the studied ground data limit the analysis, especially in mountainous regions. A good option would be to expand the dataset by choosing larger time periods and different years to compare changes in the landscape. This would be good not only for seasonal analysis but also for inter-annual analysis and observations of climate change in mountain regions. Making a comparison month per month, or image per image, require additional time, but would provide a time series analysis and a more useful information about seasonality of wet snow cover.

7. Conclusion and recommendations :

Throughout this study, Sentinel-1 mission has been confirmed to be a powerful tool in monitoring the environment, and, in this particular case, in detecting and creating wet snow cover maps. The observation of intra-annual changes in the mountain snow packs is essential to determine the seasonal impact of these changes on risks and disaster management, on the hydrology, agriculture and the landscape, central for the economy of the region. Moreover, wet snow can be an indicator of climate change and has important hydrological and ecological influences, thus, monitoring seasonal snow cover changes has been an important topic for a long while.

Remote sensing using SAR satellites offers a series of advantages respect to normal remote sensing, because provides regular time series of detections in all water conditions, i.e. it is not influenced by clouds; and it is an active radio detection sensor which transmits, from an antenna, some electromagnetic pulses and receives the echoes of the backscattered signal. Through the Doppler effect, it can precisely identify the target distance and distinguish objects on the ground, by measuring the time difference between the transmitted pulse and the reflected one.

Moreover, it is sensitive to dielectric properties of targets, so it can detect the moisture and roughness of the surface in the scene it observes.

Sentinel-1 missions offer time series images from repeat observations of the same scene and, this study, presents the potential of S1A satellite in detecting the wet snow cover with C-band SAR system. For land monitoring the Interferometric Wide Swath (IW) mode is the most suitable and commonly used because it provides a continuous coverage of the ground with a 250 km swath width.

The open access on the data allows an easier exploitation and manipulation. The Sentinel Application Platform (SNAP) is an open source software made available to the public by the EEAs Organization on the Copernicus mission web page. Unfortunately, the software requires very powerful computer processor and large memory capacity because it saves and stocks new different files after each manipulation. Manipulations has a establish sequence and order, i.e. it is impossible

to stack different images after the geocoding process. Thus, it is essential to establish the correct methodology at the beginning of the analysis in order to not to waste in vain time and efforts. Difficulties may be found also due to the size of the file (i.e. big files) and the loss of data which would constraint the analysis, demanding to restart again the process, and this would take extra time during the analysis. Images manipulation with SNAP is time taking and the optimization of procedures, through a model builder, is not always possible due to the loss of data. However, a large and helpful user community can be found in internet to help in solving problems.

The methodology employed is the Nagler's methodology [19], with the integration of Professor Small's radiometric terrain-flattening normalization, which aims to integrate terrain variations by converting values directly from the beta naught β^0 into radiometrically terrain corrected backscatter, γ_T^0 . This process is necessary in mountain regions because it avoids the issue related to the angular dependence of the backscatter and allows comparison among different images of the same scene. So, 12 high resolution Sentinel-1A images, dating from January 2019 to June 2019, in IW VV&VH polarization where combined with the ascending and the descending pathway and employed to map wet snow cover in the Swiss Alps, i.e. Berner Alpen. The cross polarization offered by S1A is the most suitable in mountain regions where topography is steep; multi-polarized images have been widely used for wet snow mapping to provide robust and accurate results.

Results show the melting process in the study area starting from March, reaching its maximum on May, and continuing in June with an evaporation event. The change in the snow pack is presented in both forms, with spatial distribution in the images where wet snow cover appears through darker pixels and with the transformations of the backscatter values in the histograms. A diachronic RGB composition has also been presented to show the difference between the chosen periods of the year (i.e. January, April and June). Finally, binary wet snow cover maps have been created to show seasonal changes in water content in the snow pack.

In conclusion, this study demonstrates the pertinent capability of the Sentinel-1 missions to detect wet snow cover in mountain regions. However, improvements can be made by integrating other forms of data to be compared with the SAR remote sensing results in order to provide more accuracy. Different satellite missions can be employed to better classify the kind of snow cover, as Sentinel-1 missions are unable to distinguish dry snow cover to bare ground; and field work dataset can be useful to improve the wet snow cover by providing more surface parameters and snow properties.

8. Remarks about the internship :

The internship at the GRID-Geneva has been a good experience for me to learn more about remote sensing techniques and, in particular, to learn about the remote sensing with RADAR, which is not part of the certificate courses. This additional knowledge is important because is complementary with standard remote sensing based on the visible part of the electromagnetic spectrum; and it allows to a deeper analysis of the snow pack cover. Since the standard remote sensing provides a good classification of the land surface, radar remote sensing can provide a further classification within the categories of the land cover, i.e. distinguish the wet snow cover to the dry snow cover.

During the five months of my internship, I had the opportunity to work in a multicultural and multi-expertise work environment which offers possibilities of learning and be trained on multiple aspects and fields of the Geographical Information Systems (GIS). Moreover, I had the chance to meet the Professor David Small, a senior research scientist at the University of Zurich, who is an expert of radar remote sensing and he suggested me to make my analysis more accurate by applying the radiometric terrain-flattening normalization in my methodology.

Therefore, I totally recommend to get the opportunity to do an internship at the GRID-Geneva to all geomatics students and also to the environment sciences students, because, the GRID-Geneva, it aims to monitor environmental issues and phenomena by transforming data in useful information and knowledge, and it offers, to students, technical expertise and knowledge about environmental issues not only at local or regional scale, but also at international level.

However, radar remote sensing analysis requires high performant technologies, e.g. powerful processors and wide memory, in order to be completely successful. During this internship about the use of radar remote sensing to detect the wet snow cover in mountain regions, I employed not only SNAP software to analyse the available data, but also software like GRASS and ArcGIS. This internship would not have been possible without some knowledge of the basic concepts and principles of the remote sensing. The certificate of geomatics offers, in these terms, a good background and important notions about GIS, teaching students theory and practise, trough software such as ArcGIS, QGIS and GRASS which have been essential for this study.

9. References :

[1] UN Environment / GRID- Geneva, “GRID - Home.” [Online]. Available: https://unepgrid.ch/en. [Accessed: 07-Jan-2020].

[2] G. Rondeau-Genesse, M. Trudel, and R. Leconte, “Monitoring snow wetness in an Alpine Basin using combined C-band SAR and MODIS data,” *Remote Sens. Environ.*, vol. 183, pp. 304–317, Sep. 2016.

[3] NASA, “Remote Sensors | Earthdata,” *Earthdata*, 2018. [Online]. Available: https://earthdata.nasa.gov/learn/remote-sensors. [Accessed: 08-Oct-2019].

[4] N. M. Donoghue, “Remote sensing,” *Prog. Phys. Geogr.*, vol. 23, no. 2, pp. 271–281, 1999.

[5] A. Moreira, P. Prats-Iraola, M. Younis, G. Krieger, I. Hajnsek, and K. P. Papathanassiou, “A tutorial on synthetic aperture radar,” *IEEE Geosci. Remote Sens. Mag.*, vol. 1, no. 1, pp. 6–43, 2013.

[6] R. Bamler, “Principles of synthetic aperture radar,” *Surv. Geophys.*, vol. 21, no. 2–3, pp. 147–157, 2000.

[7] S. W. W. Mccandless and C. R. Jackson, “Chapter 1 . Principles of Synthetic Aperture Radar,” *SAR Mar. User’s Man.*, pp. 1–23, 1978.

[8] S. Wang, B. Yang, Y. Zhou, F. Wang, R. Zhang, and Q. Zhao, “Snow cover mapping and ice avalanche monitoring from the satellite data of the sentinels,” in *International Archives of the Photogrammetry, Remote Sensing and Spatial Information Sciences - ISPRS Archives*, 2018, vol. 42, no. 3, pp. 1765–1772.

[9] N. Baghdadi, J. P. Fortin, and M. Bernier, “Accuracy of wet snow mapping using simulated radarsat backscattering coefficients from observed snow cover characteristics,” *Int. J. Remote Sens.*, vol. 20, no. 10, pp. 2049–2068, Jan. 1999.

[10] A. Heilig, A. Wendleder, A. Schmitt, and C. Mayer, “Discriminating wet snow and firn for alpine glaciers using sentinel-1 data: A case study at Rofental, Austria,” *Geosci.*, vol. 9, no. 2, p. 69, Jan. 2019.

[11] R. Solberg *et al.*, “Remote sensing of snow wetness in Romania by Sentinel-1 and Terra MODIS data,” *Rom. J. Phys.*, vol. 62, 2017.

[12] H. Chen, “Wet Snow Mapping in Southern Ontario with Sentinel-1A Observations,” 2018.

[13] Copernicus, “Sentinel-1 SAR - Technical Guide - Sentinel Online,” *Eur. Sp. Agency*, pp. 2–3, 2018.

[14] G. Giuliani *et al.*, “Building an Earth Observations Data Cube: lessons learned from the Swiss Data Cube (SDC) on generating Analysis Ready Data (ARD),” *Big Earth Data*, vol. 1, no. 1–2, pp. 100–117, Dec. 2017.

[15] B. Killough, “CEOS land surface imaging analysis ready data (ARD) description document,” 2016.

[16] E. Honeck, R. Castello, B. Chatenoux, J. P. Richard, A. Lehmann, and G. Giuliani, “From a vegetation index to a sustainable development goal indicator: Forest trend monitoring using three decades of earth observations across Switzerland,” *ISPRS Int. J. Geo-Information*, vol. 7, no. 12, Nov. 2018.

[17] M. Jauvin, Y. Yan, E. Trouvé, B. Fruneau, M. Gay, and B. Girard, “Integration of corner reflectors for the monitoring of mountain glacier areas with Sentinel-1 time series,” *Remote Sens.*, vol. 11, no. 8, p. 895, Apr. 2019.

[18] T. Nagler, H. Rott, E. Ripper, G. Bippus, and M. Hetzenecker, “Advancements for snowmelt monitoring by means of Sentinel-1 SAR,” *Remote Sens.*, vol. 8, no. 4, 2016.

[19] T. Nagler and H. Rott, “Retrieval of wet snow by means of multitemporal SAR data,” *IEEE Trans. Geosci. Remote Sens.*, vol. 38, no. 2 I, pp. 754–765, 2000.

[20] F. Filipponi, “Sentinel-1 GRD Preprocessing Workflow,” *Proceedings*, vol. 18, no. 1, p. 11, Jun. 2019.

[21] D. Small, “Flattening gamma: Radiometric terrain correction for SAR imagery,” *IEEE Trans. Geosci. Remote Sens.*, vol. 49, no. 8, pp. 3081–3093, Aug. 2011.

[22] L. Valenti, D. Small, and E. Meier, “Snow cover monitoring using multitemporal ENVISAT/ASAR data,” in *EARSeL Workshop Special Interest Group Land Ice and Snow (LISSIG) on Remote Sensing of Snow and Glaciers*, 2008, p. 8.

[23] R. Magagi, M. Bernier, and M. C. Bouchard, “Use of ground observations to simulate the seasonal changes in the backscattering coefficient of the subarctic forest,” *IEEE Trans. Geosci. Remote Sens.*, vol. 40, no. 2, pp. 281–297, Feb. 2002.

[24] D. Small, N. Miranda, T. Ewen, and T. Jonas, “Reliably flattened backscatter for wet snow mapping from wide-swath sensors,” in *ESA Living Planet Symposium*, 2013, no. 1, pp. 1–8.

[25] E. Malnes and T. Guneriussen, “Mapping of snow covered area with Radarsat in Norway,” in *International Geoscience and Remote Sensing Symposium (IGARSS)*, 2002, vol. 1, pp. 683–685.

10. Annexes :

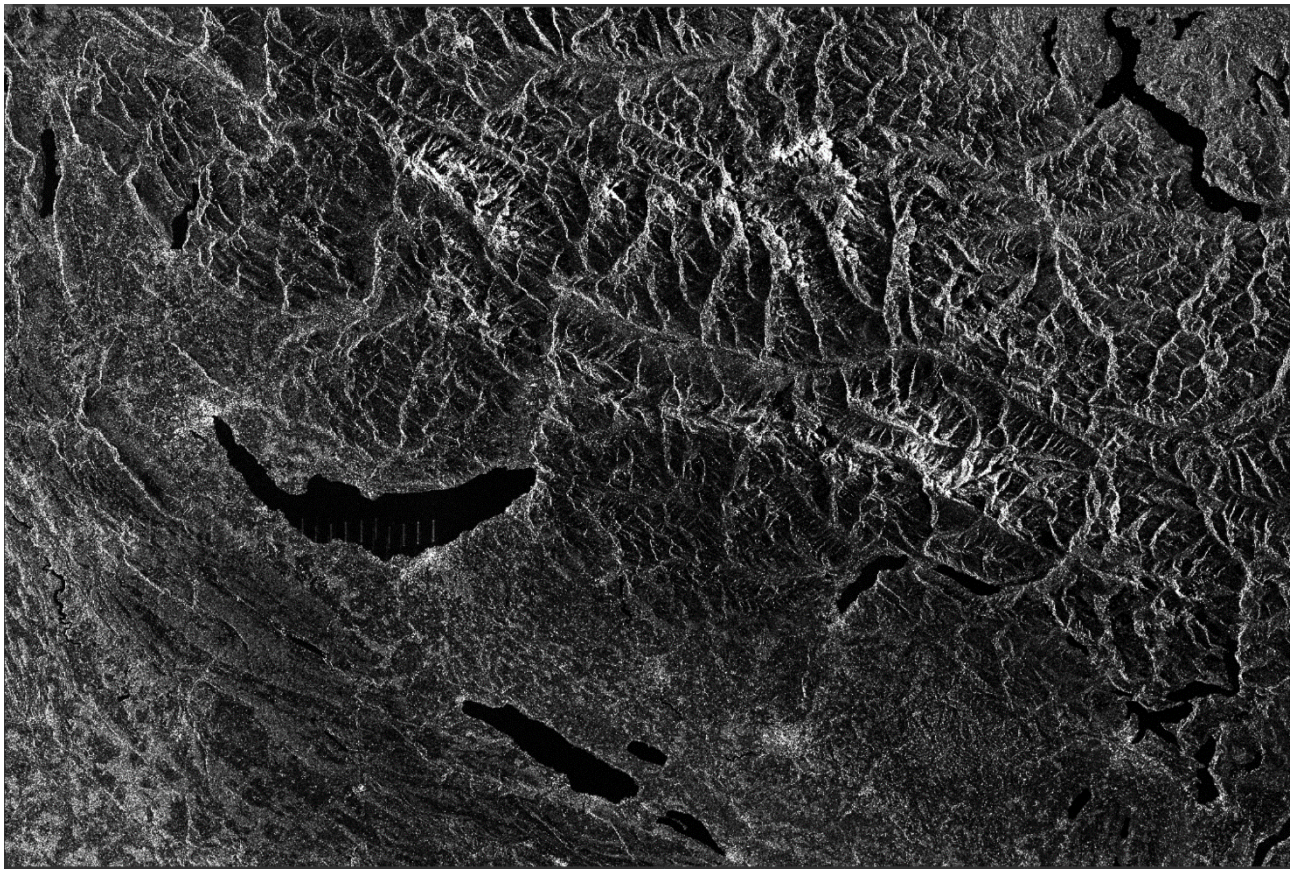

Figure 27: Example of calibrated images for the relative orbit scene numbered 88, before the terrain-flattening normalization and the geocoding.

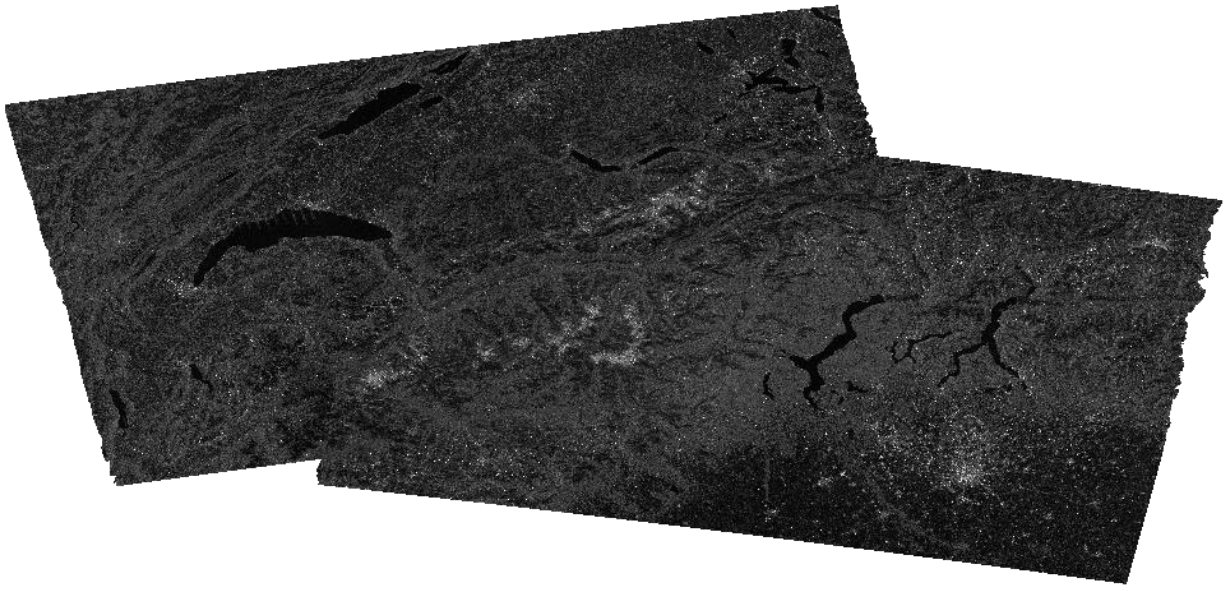

Figure 28: Example of mosaic composition where ascending and descending scenes were merged according to their geolocation. The mosaic composition causes a significant loss in the spatial resolution of the images.

Relative orbit scene numbered 66:

a)

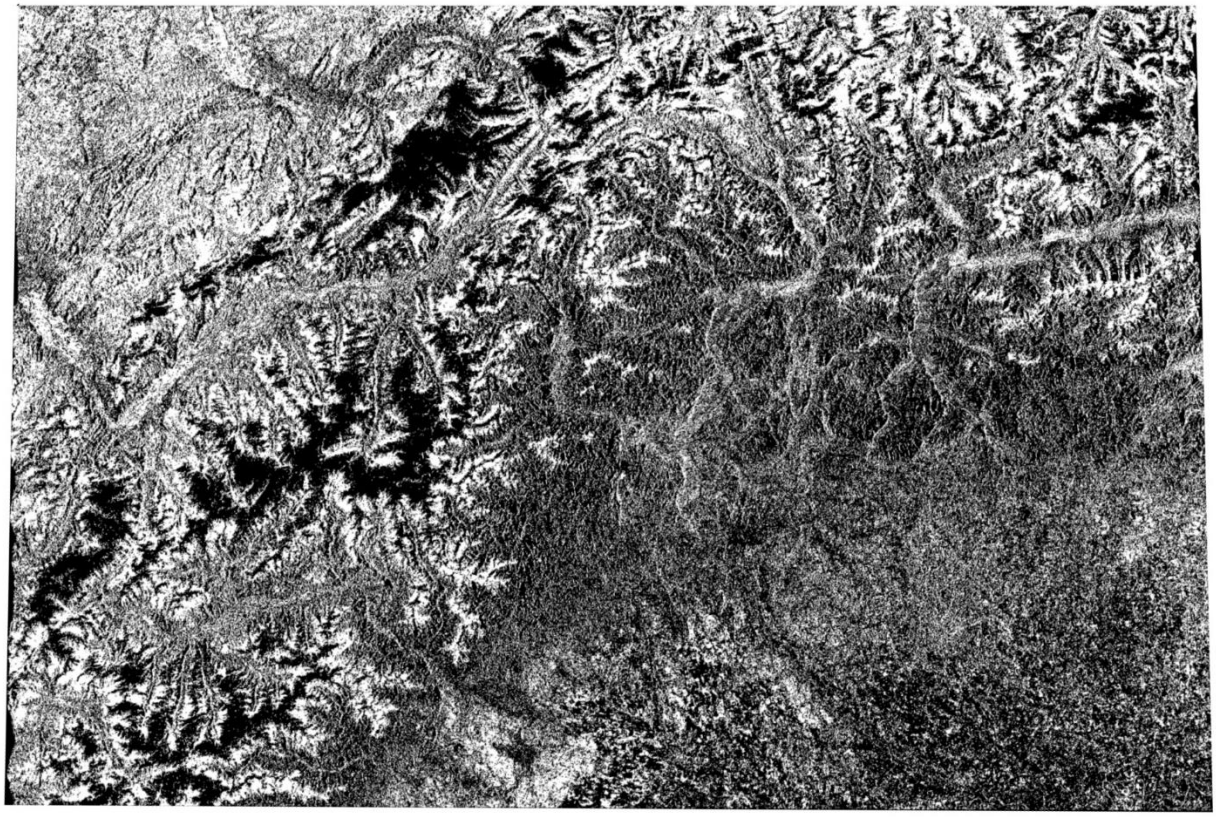

b)

Relative orbit scene numbered 88:

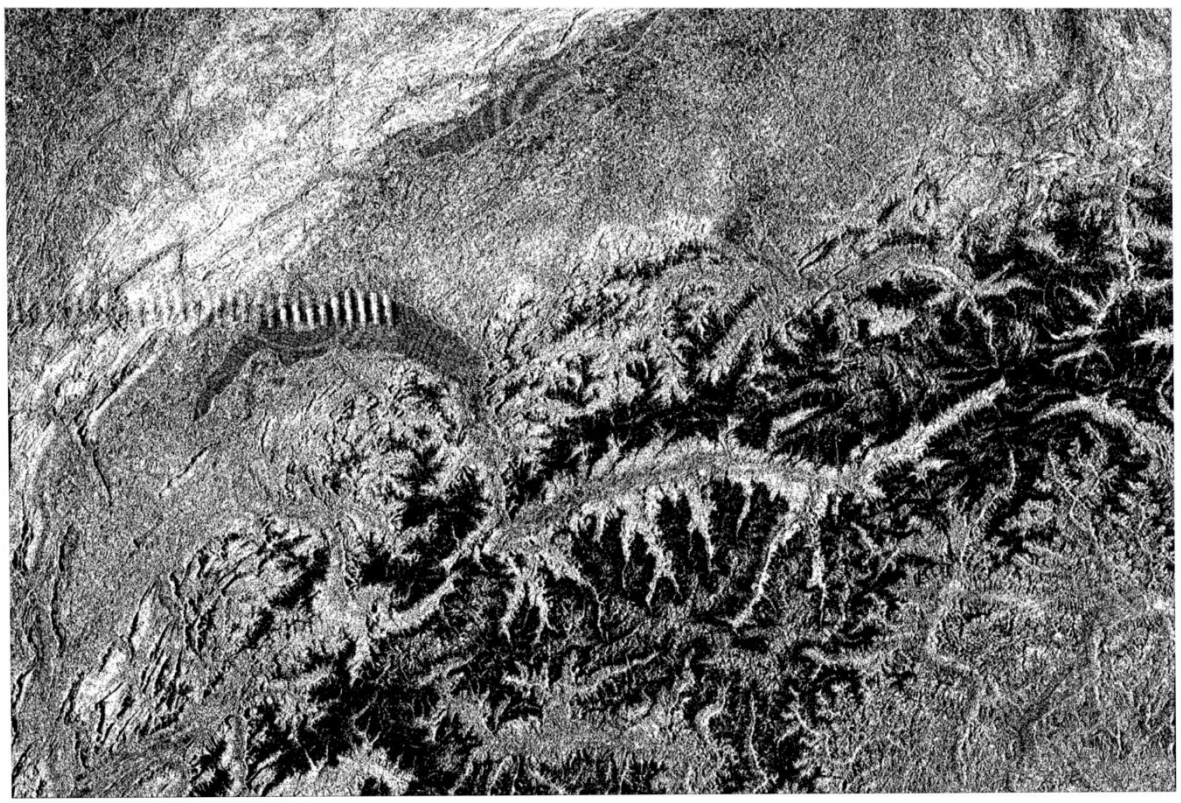

a)

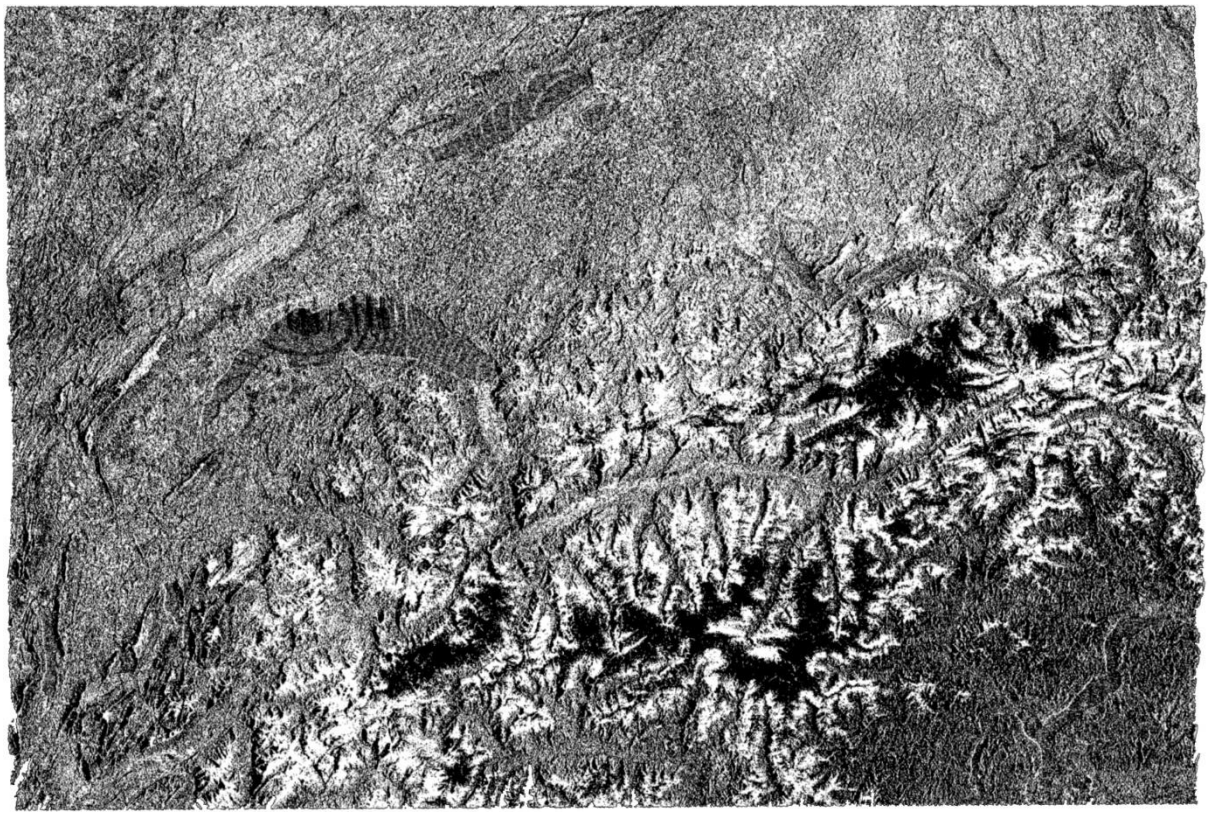

b)

Figure 29: Some representative images for the differences among the images in dB values. Wet snow cover is presented in black pixels in both scenes, at the end of April (a) and on June (b).